

Architecture of Late Orogenic Plutons in the Araçuaí-Ribeira Fold Belt, Southeast Brazil

C.M. Wiedemann^{1,2*}, S.R. de Medeiros³, I.P. Ludka², J.C. Mendes² and J. Costa-de-Moura²

¹ IMPG – Institut für Mineralogie, Petrologie und Geochemie der LMU, Theresienstr. 41/111, M-80 333, University of Munich, Germany, E-mail: wiedeman@petro1.min.uni-muenchen.de

² Department of Geology, IGEO – Federal University of Rio de Janeiro – UFRJ, Brazil, E-mail: proj-es@igeo.ufrj.br, silviar@unb.br

³ Institute of Geosciences, University of Brasília (UnB), Brasília, D.F., 70, 910-970, Brazil

*CAPES and National Research Council (CNPq)

(Manuscript received February 22, 2001; accepted July 16, 2001)



Abstract

Post-collisional to late orogenic magmatism (580 to 480 Ma) in the Araçuaí-Ribeira Fold Belt, SE Brazil, is characterized by the predominance of high-K metaluminous, allanite-titanite-bearing granitoids. Small lenses of coronitic gabbro, anorthosite, pyroxenite and phlogopite-peridotite are also common in deeper exposed areas of this fold belt. In the region of southern Espírito Santo State, the deep erosional level associated with a steep topography reveals the internal architecture of the intrusions: a tendency to funnel-shaped bodies, with sub-vertical hemi-ellipsoidal/conical roots changing upwards to shallow-dipping tops. Associated stocks, sills and dykes of basic and acid rocks generally intrude the enclosing gneisses along the foliation planes, local ductile shear zones and parallel to fold hinges. The contact between intrusions and the enclosing rocks is sharp in deeply eroded plutons e.g., Santa Angélica, Venda Nova, Mimoso do Sul and Várzea Alegre, but at shallow levels e.g., Castelo, Pedra Azul and Conceição de Muqui agmatic stoping zones occur along the borders. A magmatic foliation within the granitoids is usually well marked, but the schistosity in the surrounding gneisses wraps around the plutons. The intrusions have a bimodal chemical distribution and generally are reversely zoned with mafic cores (gabbro, diorite to tonalite) surrounded by a mingled (marble cake) zone where basic and acid rocks are interfingered, and an external zone of syenomonzonite and granite. Widespread evidence of mingling and mixing between contrasting magmas of gabbroic and granitic and/or syenomonzonitic compositions is characteristic for all intrusive complexes.

We suggest that replacement of lithospheric mantle by hot asthenospheric mantle induced partial melting of the crust. The mantle exchange was due to lithospheric mantle delamination and slab breakoff following collisional orogenesis. The bimodal plutons result from interaction among the contrasting magmas. Ascent and emplacement followed older regional structures, such as regional fold hinges and ductile shear zones.

Key words: Pluton architecture, magma mingling, late-orogenic magmatism, calc-alkaline plutons, SE Brazil.

Introduction

The classical idea of diapirism for the ascent of granitic magmas has been questioned in the last decade by Clemens and Mawer (1992) and Petford et al. (1994), among others, who strongly favor granitic magma ascent through dykes along fractures and/or pre-existing faults. Weinberg and Podladchikov (1994) pointed out the inefficiency of dyking, especially in the lower crust. They suggested a mixed model with diapirism in the lower to middle crust and dyking at shallower crustal levels. In the lower crust pervasive migration gives rise to sills,

which intrude along the regional foliation. Weinberg (1999) proposed an alternative mechanism for magma migration in hot country rocks: magma wedging of low viscosity country rocks. Several authors have showed that magma may be driven by buoyancy and coeval tectonic deformation. This is the deformation-enhanced ascent of Brown (1994, 1995), Collins and Sawyer (1996) and Brown and Solar (1999), which is also called tectonic pumping. One of ways we may address this question is through the detailed mapping and geochronology of granitic bodies. Other authors have emphasized the importance of determining the 3-D shape of igneous

intrusions, to understand the evolution of granites (e.g., Hongan et al., 1998; Roig et al., 1998; Castro and Fernández, 1998). In this paper we present detailed geological maps, sections, and field relations of six post-collisional, late-orogenic, Brasiliano plutons that crop out in the state of Espírito Santo, along the SE Brazilian Araçuaí-Ribeira Fold Belt. We review geochemical and geochronological data for these intrusions from the literature. Using these data, we consider the likely 3-D form of these plutons and speculate about likely ascent mechanism for the parent magmas.

Geological Setting

The igneous complexes considered in this paper intrude high-grade gneisses with the following parageneses: garnet-biotite-plagioclase-microcline-quartz, garnet-cordierite-sillimanite-biotite-oligoclase/andesine-microcline and hypersthene-augite-andesine/labradorite ± garnet-quartz-hornblende-biotite. These parageneses indicate high amphibolite and granulite facies,

metamorphism of metasedimentary rocks and granitic intrusions in the lower to middle crust.

The Araçuaí-Ribeira Belt is a segment of the Brasiliano-Pan-African orogenic system that includes the West Congo, Kaoko, Dom Feliciano, Damara and Gariep Belts (Pedrosa Soares et al., 1998; Pedrosa-Soares et al., 2001). Along the northern portion of the Araçuaí Belt, the structural trend follows a N-S direction. At its southern boundary, the structural trend inflects from NE to NNE, where it becomes the Ribeira Belt from 21° S southward (Figs. 1a and 1b). This gentle inflection is also traced by magnetic and gravity anomalies (Fig. 1a; e.g., Tuller, 1993). Pedrosa-Soares and Wiedemann-Leonardos (2000), based on the change of structural trend, called Araçuaí Belt the region north of 21° S, which is dominated by a N-S trend. South of 21° S the Ribeira Belt extends southwards, following the NE-SW trend (e.g., Machado et al., 1996).

Plutons are an important part of the geological framework of the Araçuaí-Ribeira Belt and were better recognized from magnetometric studies (Fig. 1; Bosum, 1973) and remote sensing (Meneses and Paradella, 1978).

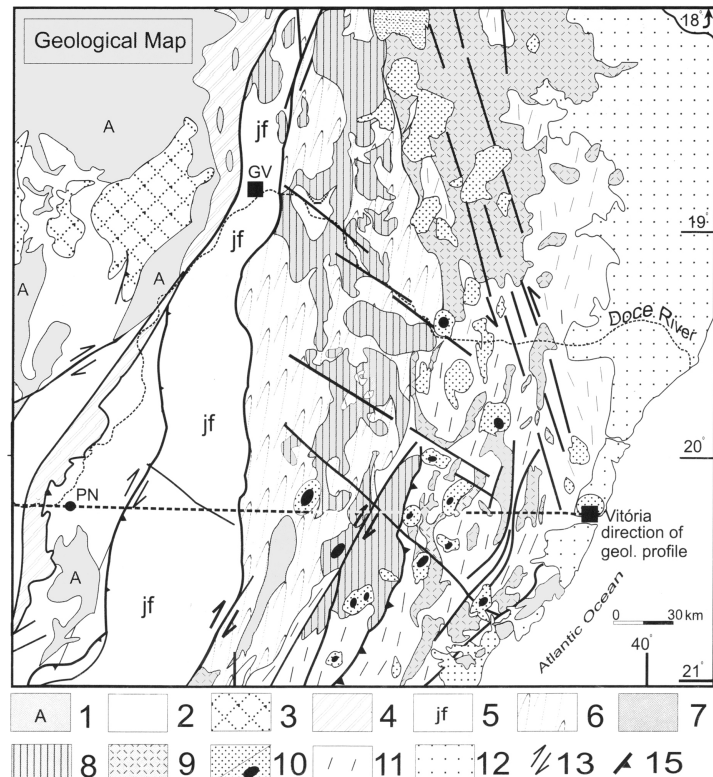
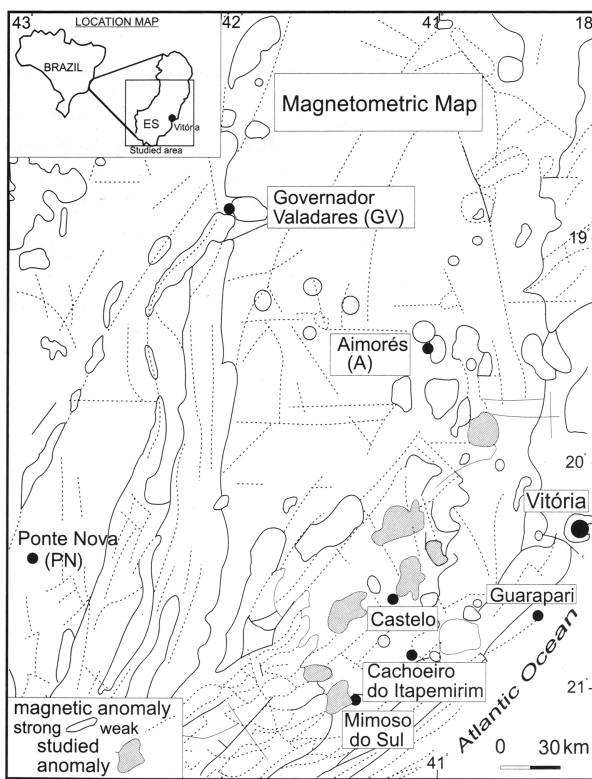


Fig. 1. Magnetometric map from the southern Araçuaí Belt (from Tuller, 1993), Geological map of the southern Araçuaí Belt and cratonic surroundings, highlighting the Neoproterozoic units (modified from Pinto et al. 1998, and Pedrosa-Soares and Wiedemann-Leonardos, 2000). 1-Archean meta-sediments, 2-TTG complexes, with greenstone belts remnants and metasedimentary units, 3-Paleoproterozoic Borrachudos Granitoid Suite, 4-Salinas Formation metavolcanic-sedimentary unit (correlated to Dom Silvério Group), 5-Juiz de Fora Complex, 6-Rio Doce Group, 7-granulite facies domain of Parába do Sul Complex. Late Paleoproterozoic and Mesoproterozoic; Late Neoproterozoic to Cambrian Granitoid suites: 8-I-type G3-I, 9-S-type G3-S and G2. Late Cambrian to Ordovician Granitoid suites: 10-I-type G5 (black dots in plutons with mafic cores), 11-high-amphibolite facies domain of Parába do Sul Complex, 12-Phanerozoic Covers, 13-Magnetometric anomalies of the studied plutons, 14-oblique to strike-slip faults or ductile shear zones, 15-thrust and detachment faults or ductile shear zones. Cidades: GV-Governador Valadares, PN-Ponte Nova, V-Vitória. Geologic section cutting the Araçuaí Belt (marked in the geological map) in depicted on figure 3. References in the text.

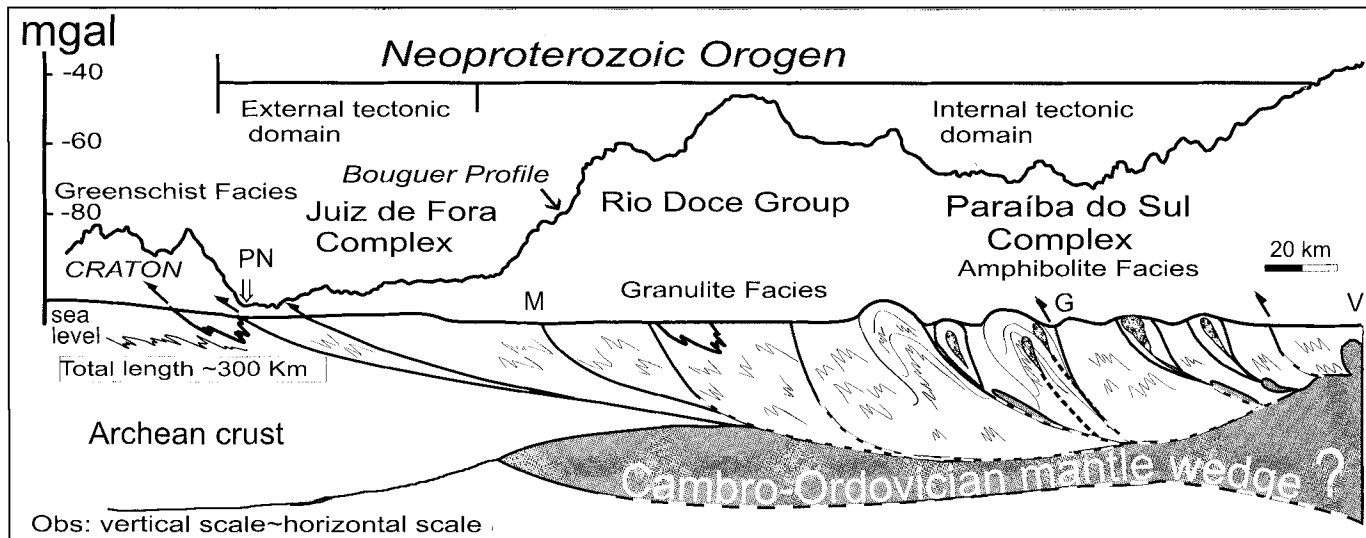


Fig. 2. Geologic section and a Bouguer profile (from Haralayi and Hasui, 1982) cross-cutting the Araçuaí Belt in Espírito Santo (references in text): external and internal tectonic domains along the Belo Horizonte (BH) to Vitória (V) section. In this section, the intrusive bodies of the Cambro-Ordovician G5 suite, are highlighted: L-Lajinha, PA-Pedra Azul, e VN-Venda Nova plutons. The enclosing rocks belong to the Dom Silvério Group and Rio Doce Groups, to the Paraíba do Sul Complex (high-amphibolite and granulite facies) and to the Juiz de Fora Complex; C-serra do Caparaó; The Geological map on figure 1 shows the direction of this section and the enclosing units. Major steeply-dipping shear zones are mostly dextral. PN-Ponte Nova, AC-Abre Campo, G-Guaçuí, M-Manhuaçu. On the Bouguer section, note the negative anomaly corresponding to the crustal thickening zone, in the internal tectonic domain.

Neoproterozoic to Cambrian granitic plutonism is widespread along the internal tectonic domain of this Brasiliano Belt (Fig. 2). Two distinct subdomains are recognized in the internal domain: a northern subdomain (north of 19°S), where the anatetic zone of the orogen is better exposed (Fig. 3) and a southern subdomain characterized by prominent steeply-dipping, dextral shear zones, granulite facies rocks and granitic plutons with mafic cores (Fig. 1). The southern subdomain is granulitic and preserves the deepest crustal levels of the orogen (Seidensticker and Wiedemann, 1992; Söllner et al., 2000) and the plutonic structures highlighted in this work intrude this subdomain. The southern Araçuaí Belt is characterized by NE-trending, dextral transpressive shear zones, which are an extension of those from the northern Ribeira Belt (Fritzer, 1991; Machado et al., 1996; Cunningham et al., 1998; Heilbron et al., 1998). Nevertheless, thrust tectonics remains the more important regime within the Araçuaí frame (Pedrosa Soares et al., 2001).

Regional Deformation and Metamorphism

The main collisional stage of the Brasiliano Araçuaí-West-Congo Orogen in this region occurred ca. 600–580 Ma (Sm–Nd whole-rock, Fischel, 1998; U–Pb on zircons, Söllner et al., 2000). During this tectonic episode metamorphism up to high amphibolite and granulite facies overprinted older structures, and associated deformation

caused shortening of ~30–40% (Lammerer, 1987; Fig. 2). The main regional schistosity or gneissic foliation defines the structural trend of different tectonic domains. The Brasiliano deformation produced west-verging, moderately- to steeply-dipping thrusts, which are truncated by dextral, high-angle, oblique- to strike-slip shear zones, defining a prominent transpressive system (Pedrosa-Soares et al., 2001). The metamorphic banding was tightly to isoclinally folded and refolded to form long-wavelength folds, with upright to slightly west-verging axial planes and amplitudes up to 10 km (Söllner et al., 2000; Figs. 1 and 2). Such folding is associated with contemporaneous stretching parallel to the fold axes, indicating a transpressive regime (Lammerer, 1987; Fritzer, 1991; Cunningham et al., 1998). Steep shear zones were active throughout the orogen, even during the docking stage of the colliding blocks (Pedrosa-Soares and Wiedemann-Leonardos, 2000). The Guacuí lineament is considered to be the most important of the shear zones of the region (Fritzer, 1991; Cunningham et al., 1998; Figs. 1 and 2).

The Bouguer profile in figure 2 shows the limit between the external and internal tectonic domains. A large negative anomaly (≤ -100 mGal) marks the external tectonic domain, separating the gravity patterns from the cratonic region and internal tectonic domain. Gravity values gently rise in the Juiz de Fora Complex (Paleoproterozoic basement). When the Brasiliano Belt is crossed (Rio Doce Group), gravity values reach a maximum of ~ -40 mGal,

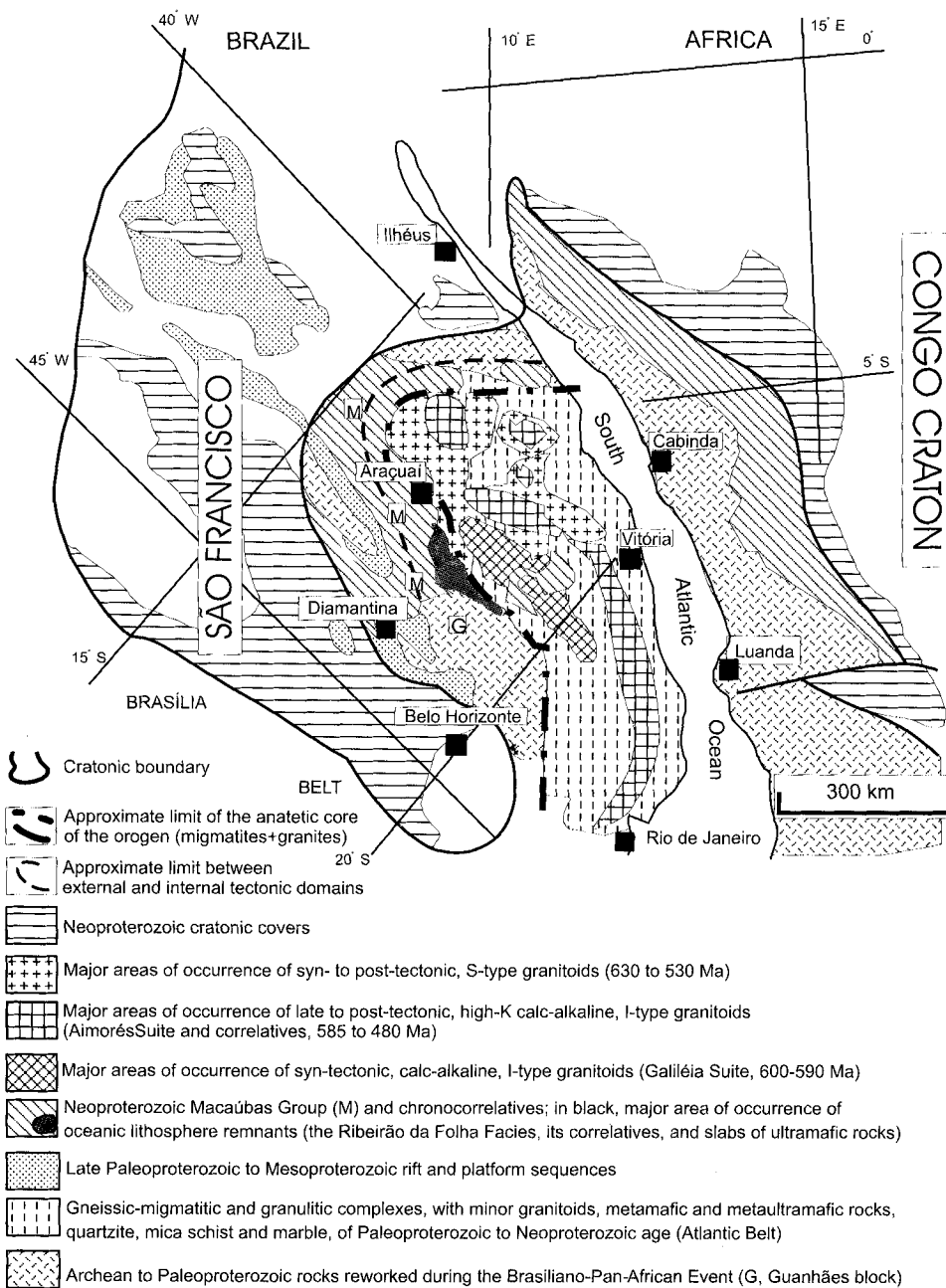


Fig. 3. Tectonic sketch map of the Araçuaí-West-Congo Orogen in a predrift reconstruction and its granitoids. Slightly modified from Pedrosa Soares et al. (1998).

implying a significant influence of high-density rocks near the surface (Fig. 2). Along the Manhuaçu shear zone, the transpressive tectonic regime has resulted in juxtaposition of slices of basic granulites of the Juiz de Fora Complex with Neoproterozoic peraluminous hypersthene-garnet-granulites and staurolite-garnet gneisses (Rio Doce Group see Costa, 1998). Geothermobarometric studies of granulites and high-amphibolite gneisses yielded metamorphic temperatures greater than 800°C and pressures around 0.8 to 1 GPa, confirming that this region exposes the deepest crustal levels of the orogen (Seidensticker and Wiedemann, 1992; Söllner et al., 2000).

East of the Manhuaçu shear zone, the pattern of alternating gravity anomalies decreases to a minimum of ~ 70 mgal, close to the Guaçuí shear zone, recording the thick metasedimentary packages of the Rio Doce Group and Paraíba do Sul Complex. In this region, the metamorphic conditions reached temperatures greater than 650°C and pressures around 0.65 to 0.75 GPa, at about 590 Ma (Seidensticker and Wiedemann, 1992). From the Guaçuí shear zone towards the town of Vitoria (Figs. 1 and 2), the gravity values increase again. Most of this increase is due to the present Atlantic oceanic crust, the presence of Paraíba do Sul granulites, exposed along

the coast, and the widespread intrusion of granitoids and mafic magmas. In the westernmost part of the Paraíba do Sul Complex, amphibolite facies garnet and horblende gneisses, sillimanite-quartzites and diopsidic-grossular-scapolite-gneisses (calc-silicates) were first metamorphosed and deformed at 589 ± 8 Ma (U-Pb on zircons; Söllner et al., 2000). Around 565 ± 9 Ma (U-Pb on zircons) this package of rocks achieved the granulite facies with crystallization of hypersthene gneisses under high CO_2 pressures, temperatures greater than 800°C and pressures around 0.65 to 0.75 GPa (Söllner et al., 2000).

Orogenic Magmatism

A profusion of late Neoproterozoic to Cambro-Ordovician calc-alkaline, I-type granitoids occur along the internal tectonic domain of the Araçuaí Belt and northern Ribeira Belt (Pedrosa-Soares and Wiedemann-Leonardos, 2000; Söllner et al., 2000; Pedrosa-Soares et al., in press; Fig. 3). They intruded around 580 Ma, shortly after the main collisional phase. The last regional deformation affects these intrusions, which as a result form large batholithic gneissic bodies (Figs. 1, 2, 3 and 4).

According to the literature, I-type (metaluminous) metagranitoids crystallized from melts derived from mixed sources, with an important contribution of an oceanic plate and/or a mantle source mixed or mingled with partial melts from a prevailing meta-igneous and minor metasedimentary crust (Pedrosa-Soares et al., 1999; Pedrosa-Soares and Wiedemann-Leonardos, 2000). S-type

suites (peraluminous) were synchronous with the intrusion of the 580 Ma I-type. They evolved from the melting of largely metasedimentary sources with only minor contribution from the partial melting of an oceanic plate or mantle source (Pedrosa-Soares et al., 1999; Pedrosa-Soares and Wiedemann-Leonardos, 2000). During the orogenic phase granitic magma intruded and crystallized while contractional deformation was active. Both groups of rocks intrude 600–590 Ma gneisses and show good similarities to the syntectonic plutons studied by Brown and Solar (1999), which are clear examples of tectonic pumping.

The Late-Orogenic Magmatism

After the collisional phase (ca. 600–580 Ma) the lower and middle crust remained hot (Söllner et al., 2000; Pedrosa-Soares et al., in press). During the 560 to 535 Ma period there was a tectonic relaxation along the entire belt, save for the deformation along the ductile shear zones and the slight refolding of the regional fold hinges in Espírito Santo (Bayer et al., 1987; Seidensticker and Wiedemann, 1992). That period was also followed by quiescence in the magmatic activity. A new magmatic episode started around 535 and lasted until 480 Ma (Söllner et al., 2000). During this period discordant dykes and ductile stretching suggest a change towards an extensive regime (Bayer, 1987; Lammerer, 1987). The plutons described in this paper were emplaced and crystallized during this late period and record the youngest post-collisional magmatic episode.

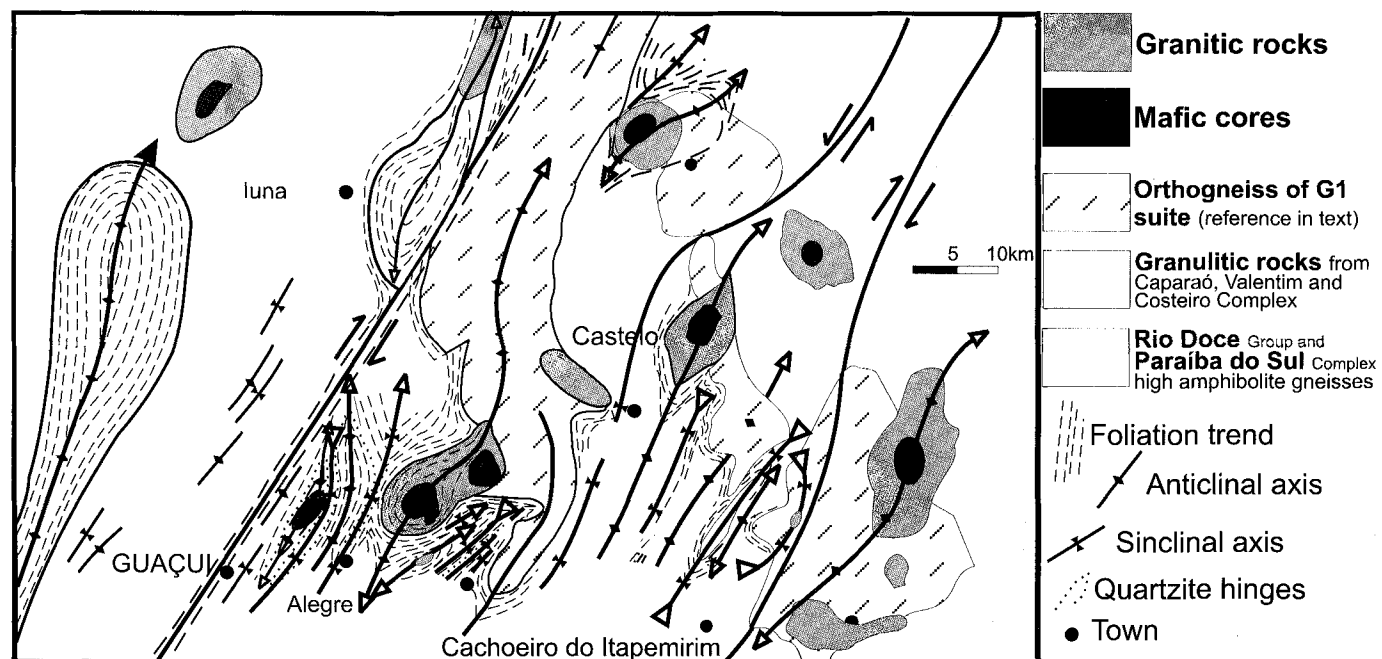


Fig. 4. Structural sketch map from South Espírito Santo (modified after Bayer et al., 1987).

Geology of the Plutons

Vertical exposures with differences in levels over 500 meters reveal the inner structure of the plutons, a fundamental information in the understanding of the shape of granitic intrusions, melt migration and emplacement in the crust. The original mapping scale for the intrusive complexes was 1: 25,000. Outcrop and map

scale information depict variable but normally steep side walls ($>70^\circ$) and internal magmatic foliations, in the complexes with large gabbroic/dioritic centers, such as Santa Angélica, Castelo, Mimoso do Sul and Várzea Alegre (Figs. 5, 6 and 7). In the complexes with large granitic to monzonitic aureoles, shallower magmatic foliations ($<70^\circ$) are more frequent (Pedra Azul and Conceição de Muqui; Figs. 6 and 7).

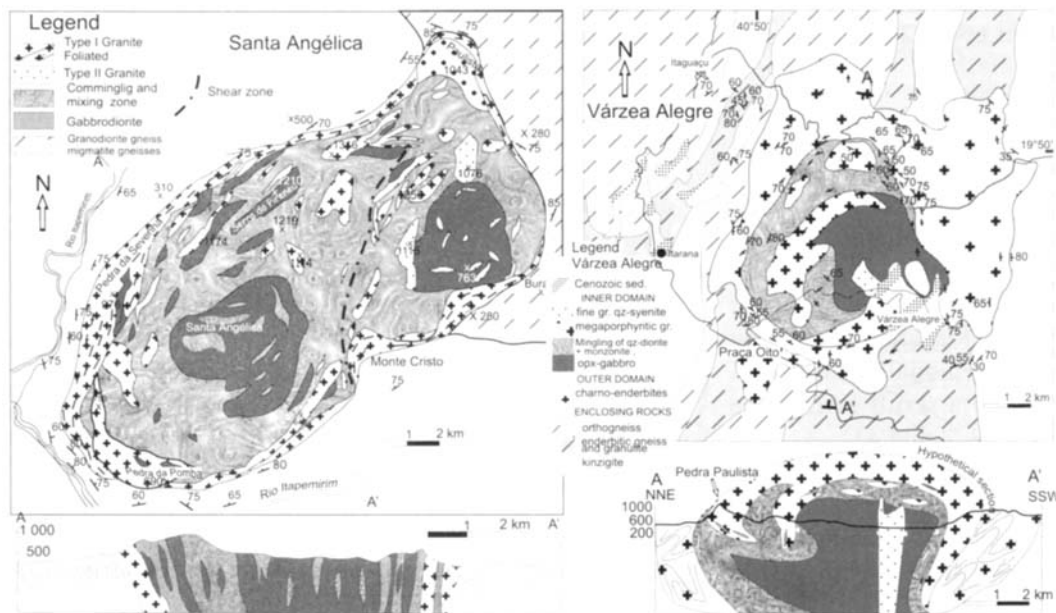


Fig. 5. Geological maps of Várzea Alegre and Santa Angélica. Geology of VAIC from Tuller, (1993) and Medeiros et al. (2000). Geology of SAIC from Bayer et al. (1987).

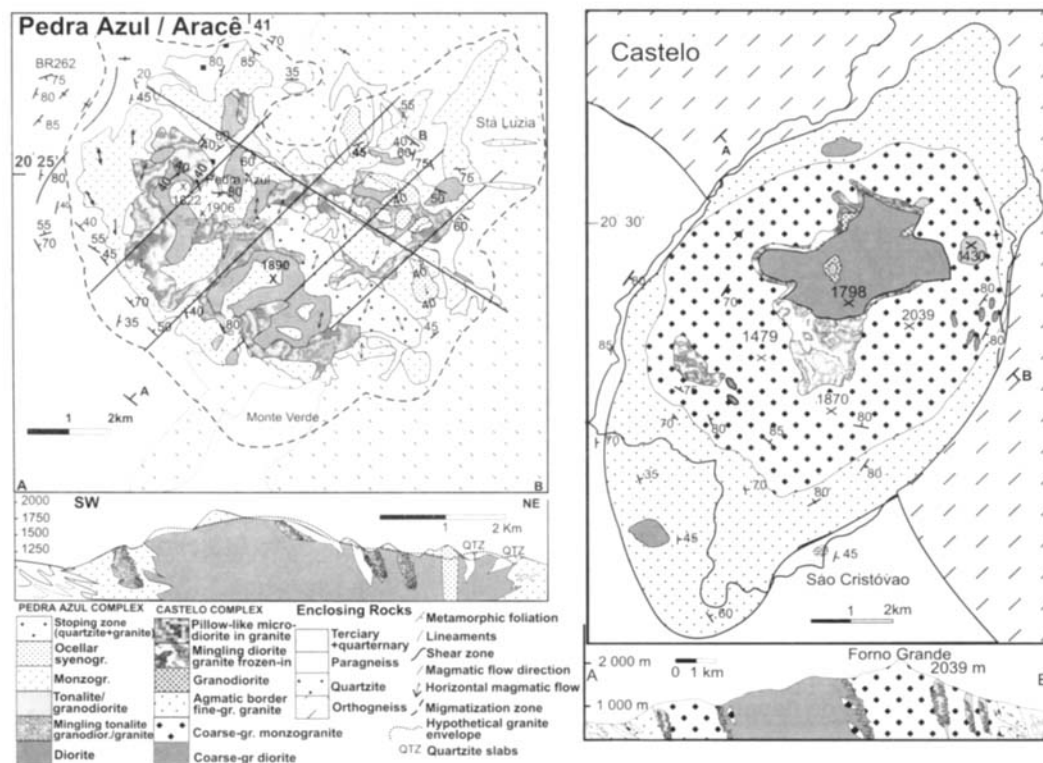


Fig. 6. Geological maps of Castelo and Pedra Azul. Geology of Castelo modified after Bayer et al. (1987) and Wiedermann et al. (1997). Geology of Pedra Azul modified after Wiedermann et al. (1997) and Costa-de-Moura et al. (1999).

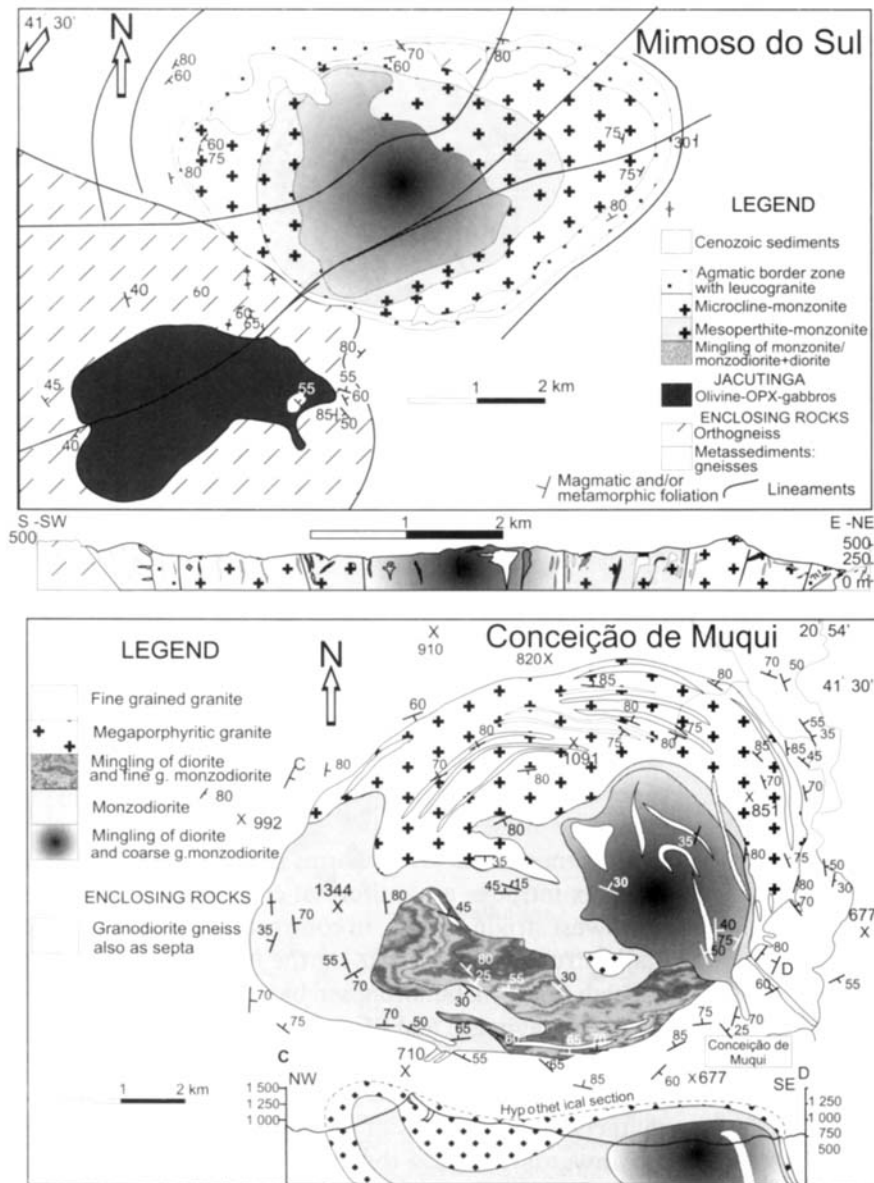


Fig. 7. Geological maps of Mimoso do Sul and Conceição de Muqui. Geology of Mimoso do Sul from Ludka (1991). Geology of Conceição de Muqui modified after Murad (1992).

Várzea Alegre

The Várzea Alegre Intrusive Complex (VAIC) is an inversely zoned multistage structure with an almost circular shape of ~150 km² (Fig. 5; Medeiros et al., 2000). According to Mendes et al. (1999) it is enclosed by a large early ring of megaporphyritic dark green charnockitic rocks. The outer domain includes hyperthene-bearing quartz-diorites, granodiorites (opdalite or charno-enderbite) and quartz-monzonites (mangerite). This outer domain varies in width from few hundred metres at the southern and western borders, to almost 4 km at the eastern and nothern borders, forming an expressive topography of 'sugar loaves'. The country rocks are ortho- and para-gneisses of high amphibolite to granulite facies with NE-SW-structural trends.

The late intrusion consists of dark gray opx-gabbro/monzogabbro at the center, surrounded by diorite/quartzdiorite-monzodiorite and light megaporphyritic granite. A latest stock of titanite-bearing syenogranite cross cuts the opx-gabbro (Medeiros et al., 2001). The contact between the megaporphyritic granite and the diorite is a mingled/mixed zone consisting of quartz-diorite and quartz-monzodiorite (Fig. 8a). The internal foliation is steep to moderate.

Geochemical data of the inner domain indicate a metaluminous, Hy-normative, silica-oversaturated magma, with high to medium contents of incompatible elements (Table 1, Figs. 9, 10, 11 and 12). Whole rock data indicate medium-K contents for the basic to intermediate rock types. The megaporphyritic

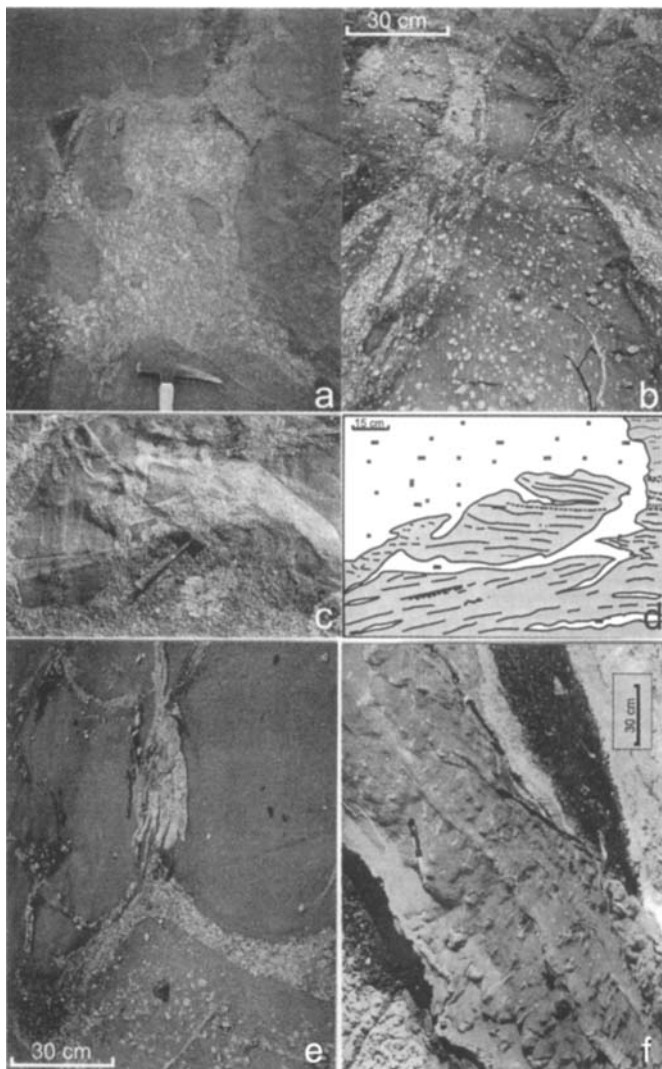


Fig. 8. Field relations. (a) Vázea Alegre – contact between felsic and mafic domains, where granitic crystal mushes surround dioritic lobate masses, (b) Santa Angélica - tightly packed heterogeneous gabbro-diorite enclave swarms in granite I (photograph of B. Lammerer), (c) Santa Angélica - fine-grained type II granite as the matrix of the agmatic border, (d) Castelo – outcrop drawing of the agmatic border formed by granite II intruding the enclosing banded gneiss, (e) Santa Angélica - granite I interfingers fine-grained diorite/gabbro, xenocrysts from the granite are mechanically introduced into the mafic magma (photograph of B. Lammerer), (f) Castelo - hybrid syn-intrusive dyke with granitic shlieren in a microdioritic matrix.

granite and the charnockitic rocks are high-K calc-alkaline.

Santa Angélica

The Santa Angélica intrusive complex (SAIC in Fig. 5) is one of the most interesting examples of the late to post-orogenic plutons in this mobile belt (Wiedemann et al., 1986; Bayer et al., 1987). The SAIC covers about 200 km² and is an elliptical-shaped intrusion composed

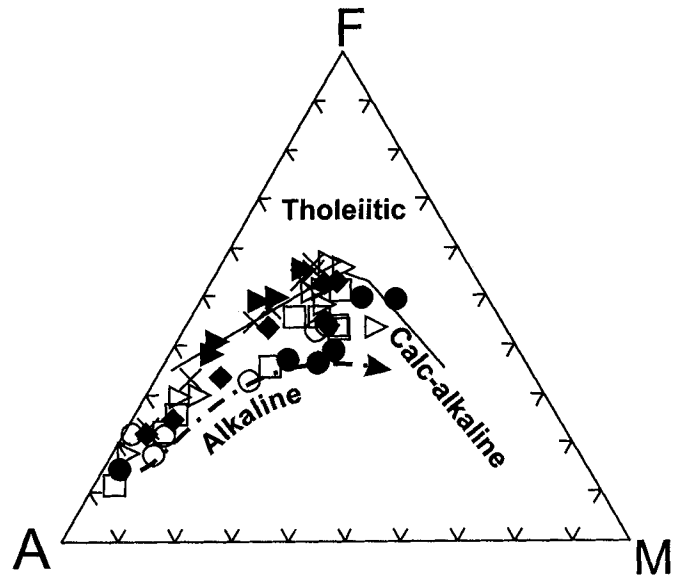


Fig. 9. ETR-diagram normalized after Sun and McDonough (1989). Symbols: Várzea Alegre square charnockite; half-filled diamond opx-gabbro; triangle qz-diorite/qz-monzonodiorite; circle megaporphritic granite; Jacutinga: half-filled diamond; Pedra Azul: diamond diorite; triangle syenogranite; circle granite.

of several roughly concentric lens-shaped granitic layers, elongated lenses of gabbro-diorite and tightly packed heterogeneous enclave swarms (Fig. 8b and 8e). The complex intrudes an antiformal cross structure with an northwest striking hinge, in contrast to the hinge lines of major structures that strike northeast. The country rocks are high-grade metamorphosed biotite-garnet-sillimanite-gneiss (paragneiss) and biotite-hornblende granodioritic to tonalitic gneiss (orthogneiss). These are locally migmatized, showing sub-vertical foliation with parallel contacts to the borders of the intrusive complex, which dip inwards towards the intrusion. The intensity of migmatization is stronger close to the pluton contact, where the enclosing gneisses exhibit nebulitic fabrics consistent with partial melting.

The foliation inside the intrusive complex is normally sub-vertical and, at map scale, the whole magmatic body appears somewhat boudinaged. This pluton shows a general inverse concentric zoning with more acidic rocks (Type I granite) at the margins, varying to a twin core of more basic rocks. Type II granite is fine-grained and intruded in a late brittle phase (Fig. 8c). Common signs of magma mingling between monzogabbros and granites can be observed throughout the intrusion (Wiedemann et al., 1986; Schmidt-Thomé and Weber-Diefenbach, 1987; Wiedemann et al., 1997). Large mingled zones formed by enclave swarms are in different degrees of hybridization with the granite (Fig. 10). A main NE-SW active shear zone (Marre, 1986) caused more intensive mingling,

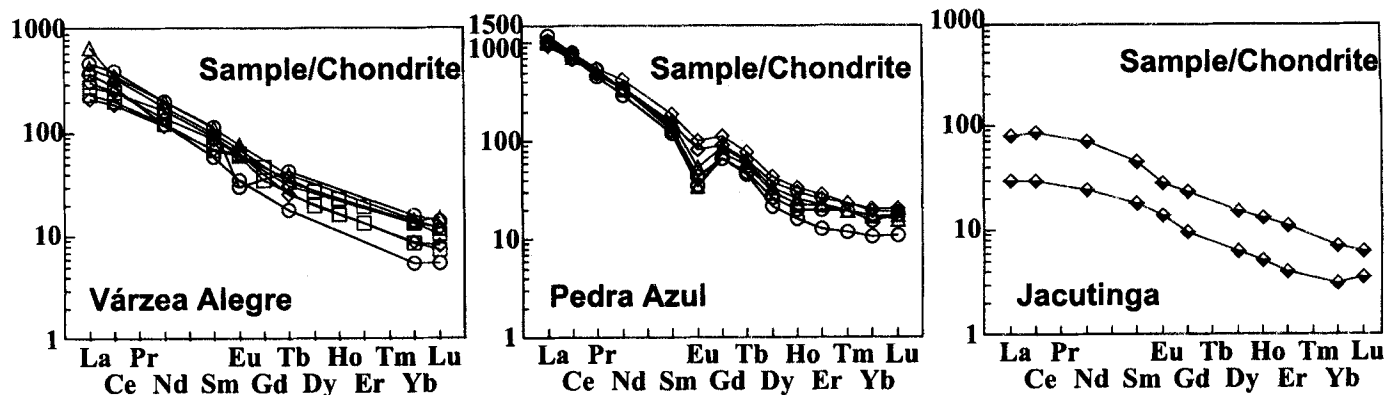


Fig. 10. AFM-diagram from Irvine and Baragar (1971) for the studied rocks. Legend: X—Pedra Azul, open circle—Conceição de Muqui, filled circle—Mimoso do Sul, losangle—Castelo, quadrangle—Santa Angélica, open triangle—Varzea Alegre inner domain, filled triangle—Varzea Alegre charnockitic outer domain.

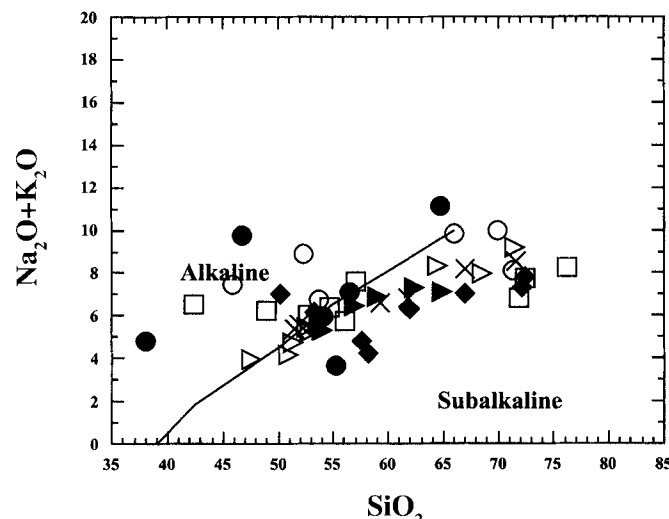


Fig. 11. $\text{SiO}_2 \times \text{Na}_2\text{O} + \text{K}_2\text{O}$ diagram (Irvine and Baragar, 1971) for the studied rocks. Legend: X—Pedra Azul, open circle—Conceição de Muqui, filled circle—Mimoso do Sul, losangle—Castelo, quadrangle—Santa Angélica, open triangle—Varzea Alegre inner domain, filled triangle—Varzea Alegre charnockitic outer domain.

producing a fine-banded rock consisting of gabbrodioritic and granitic layers. This NE-SW shear zone separates the gabbroic nuclei. Geochemical data of rocks from Santa Angélica is shown in tables 2, 3 and figures 10, 11 and 12.

According to Bayer et al. (1987), with increasing distance to the pluton the country rock foliation turns into a NNE-SSW trend. Approaching the contact to the intrusion, the country rock foliation steepens to an almost vertical position or dips beneath the intrusion. The authors interpreted the observation as evidence of diapiric emplacement.

Castelo

The Castelo Complex (Fig. 6) is an elliptical intrusion around 100 km^2 , that consists of a dioritic center and a granitic border (Table 2). The border region is over 2 km

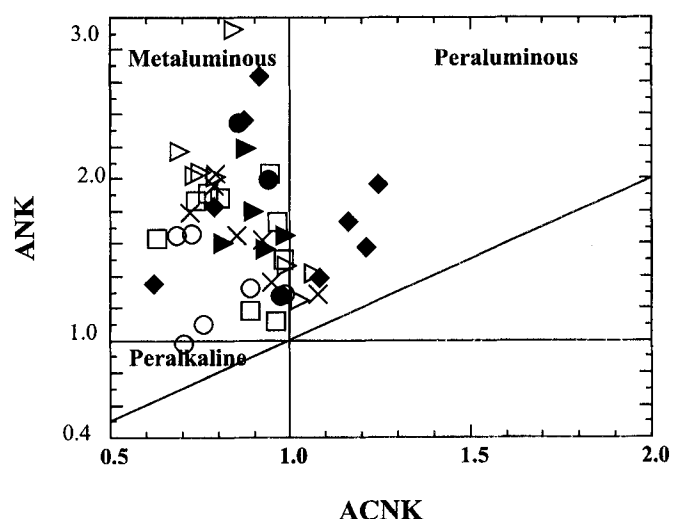


Fig. 12. A/CNK-A/NK diagram from Maniar and Piccoli (1989) for the studied rocks. Legend: X—Pedra Azul, open circle—Conceição de Muqui, filled circle—Mimoso do Sul, losangle—Castelo, quadrangle—Santa Angélica, open triangle—Varzea Alegre inner domain, filled triangle—Varzea Alegre charnockitic outer domain.

wide and consists of the interlayering of two types of granites: a megaporphyritic and a fine-grained granite. The fine-grained granite is porphyritic and titanite-bearing. It is a monzogranite, very similar to the type-II granite from Santa Angélica. It forms most of the matrix of the agmatitic border (Fig. 8d). It frequently exhibits micaceous schlieren and ghost structures from the partially assimilated gneisses. This granite II also intrudes the border gneiss as *lit par lit* sills or as discordant dykes. The contacts usually show evidence of stoping (Fig. 8d). Sharp discordant contacts with the enclosing rocks are more frequent than concordant contacts. A coarse-grained diorite forms the center of the intrusion. In this domain, linear and planar structures are less marked; on the other hand, a profusion of cross joints and associated granitic veins are typical for the region. This is an evidence of

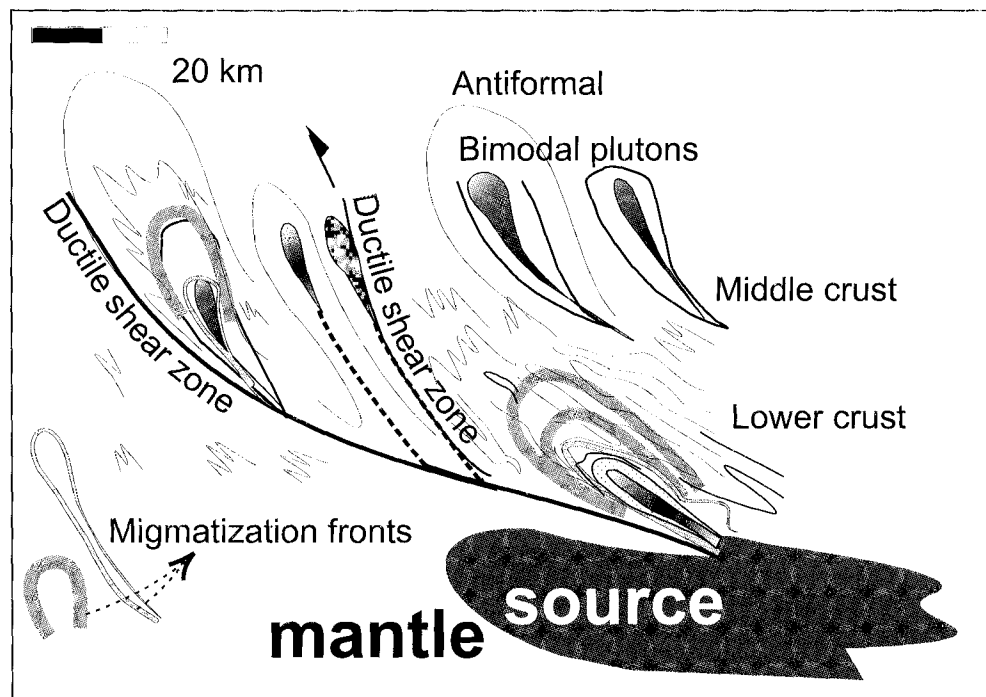


Fig. 13. Final model showing: (1) injection of mantellic wedges along deep ductile shear zones; (2) induced partial melting of the continental crust and coeval production of granitic magmas, which were channelled into the composite plutons, along the continuation of shear zones in shallower levels.

fracturing and dyking of an early consolidated dioritic core, possibly undergoing shrinkage during solidification (Wiedemann et al., 1997). At the contact between coarse-grained granite and coarse-grained diorite, a thin layer of microdiorite is present. This is formed by tightly

packed enclave swarms, which show different degrees of hybridization with the granite. In some areas the mixing between granite and diorite magma was more intense and favored formation of a hybrid granodioritic rock.

Table 1. Chemical analyses of basic, intermediate and acid rocks from Várzea Alegre.

Sample	VA-1	VA-2	VA-3	VA-4	VA-5	VA-6	VA-7	VA-8	VA-9	VA _c -1	VA _c -2	VA _c -3	VA _c -4	VA _c -5
SiO ₂	47.57	50.84	51.27	53.70	52.64	52.83	64.52	68.48	71.49	53.99	56.98	59.00	62.39	64.90
TiO ₂	2.95	1.51	3.72	2.51	2.30	2.57	1.05	0.67	0.30	1.97	1.66	1.50	0.89	0.94
Al ₂ O ₃	19.14	17.95	13.87	15.29	15.66	14.83	15.46	14.71	14.69	16.58	15.82	15.10	16.14	15.10
Fe ₂ O ₃	11.16	9.06	12.51	10.50	10.13	10.77	4.54	4.04	2.35	11.28	9.74	9.30	6.45	5.57
MnO	0.15	0.13	0.18	0.15	0.14	0.15	0.50	0.07	0.03	0.18	0.16	0.14	0.15	0.11
MgO	3.94	6.30	3.81	3.57	4.20	3.85	1.32	0.76	0.32	2.76	2.39	1.80	1.02	0.99
CaO	10.06	8.36	7.53	6.45	7.24	7.06	2.78	1.88	1.40	6.22	4.87	5.00	3.64	3.60
Na ₂ O	3.17	2.88	2.30	2.82	3.10	2.91	2.77	3.19	3.16	3.28	3.16	3.50	3.21	3.50
K ₂ O	0.77	1.30	2.42	2.75	2.37	2.35	5.55	4.74	6.05	2.02	3.33	3.40	4.14	3.60
P ₂ O ₅	1.38	0.70	2.00	1.01	1.01	1.13	0.40	0.40	0.15	0.95	0.77	0.66	0.39	0.42
RE	0.48	0.54	0.53	0.64	0.72	0.61	1.46	0.79	0.42	0.21	0.27	0.60	0.63	1.40
Total	100.77	99.57	100.14	99.39	99.51	99.06	99.90	99.73	100.36	99.44	99.15	100.00	99.05	100.13
Minor elements in ppm														
Ni	14	46	12	16	25	25	10	10	10	17	15	14	n.m.	11
Co	93	63	65	51	60	72	48	69	42	31	38	61	22	56
V	284	157	320	n.m.	195	232	69	8	15	121	107	125	43	35
Cu	31	23	29	25	28	30	13	32	43	n.m.	n.m.	n.m.	n.m.	n.m.
Zn	115	102	155	138	127	142	93	86	n.m.	169	128	134	102	101
Rb	6	27	67	90	49	52	184	212	229	36	58	64	84	79
Ba	720	1091	1300	1660	1841	1826	1836	1613	771	1746	2779	2727	2588	2246
Sr	1188	1393	684	714	1040	891	341	280	147	677	614	579	475	428
Ga	23	21	n.m.	n.m.	22	21	19	22	22	21	20	21	19	20
Nb	19.8	10.4	35.7	27.6	24.1	27.5	n.m.	33	25	46	36	35	29	36
Zr	96	109	364	435	340	368	651	359	224	1084	841	724	840	819
Y	26	18	54	42	33	36	15	48	39	36	35	36	34	29

VA = Várzea Alegre inner domain, VA_c = Várzea Alegre outer charnockitic domain.

Table 2. Chemical analyses of basic and intermediate rocks from Santa Angélica, Castelo and Pedra Azul.

Sample	SA-1	SA-2	SA-3	SA-4	SA-5	SA-6	CA-1	CA-2	CA-3	CA-4	CA-5	PA-1	PA-2	PA-3	PA-4	PA-5
SiO ₂	42.35	48.95	54.74	52.69	56.09	57.10	50.19	53.34	58.17	57.58	61.89	51.91	51.41	53.46	59.24	61.81
TiO ₂	3.39	2.45	2.11	2.44	2.11	1.29	2.96	2.64	2.18	2.18	1.74	3.10	3.11	2.73	2.15	1.62
Al ₂ O ₃	15.00	16.34	16.95	14.84	14.51	17.73	13.31	14.33	13.63	13.65	14.86	14.95	14.83	13.95	14.51	14.56
FeO	8.41	5.94	5.13	5.56	5.26	3.76	6.49	5.52	5.71	5.91	5.76	nm	nm	nm	nm	nm
Fe ₂ O ₃	5.60	3.96	3.42	3.71	3.51	2.51	4.33	3.68	3.81	3.94	1.02	12.56	12.54	11.13	9.02	7.84
MgO	6.23	5.80	3.36	5.63	4.19	3.22	5.50	5.11	3.86	3.66	2.26	3.32	3.27	2.95	2.25	1.83
CaO	8.07	6.91	5.28	6.69	5.69	4.51	6.35	5.70	5.35	5.43	2.40	6.25	6.27	6.32	4.54	3.74
Na ₂ O	3.79	3.21	2.54	2.63	2.67	3.47	3.96	2.04	0.99	0.99	1.29	2.81	2.62	2.81	2.88	2.83
K ₂ O	2.74	3.04	3.86	3.37	3.07	4.16	3.09	4.14	3.27	3.82	5.03	2.78	2.76	2.95	3.74	4.00
MnO	0.20	0.12	0.10	0.12	0.14	0.59	0.14	0.11	0.14	0.14	0.09	0.18	0.18	0.14	0.13	0.11
P ₂ O ₅	2.01	2.12	1.24	1.60	1.09	0.64	2.12	1.78	1.29	1.24	1.08	1.59	1.60	1.54	0.96	0.70
LOI	0.34	0.60	0.46	0.70	0.98	0.95	0.65	0.84	0.90	0.72	2.13	0.49	0.49	0.51	0.34	0.57
Total	98.13	99.44	99.19	99.98	99.31	99.93	99.09	99.23	99.30	99.26	99.55	99.95	99.08	98.50	99.76	99.61
Minor elements in ppm																
V	654	333	286	243	162	160	349	178	281	279	49	166	166	167	108	90
Cr	55	65	44	106	48	29	79	152	66	44	37	32	34	39	25	24
Co	36	34	35	20	9	30	24	4	25	24	28	37	38	49	27	35
Ni	23	42	21	55	35	21	66	115	37	34	22	26	27	25	17	16
Cu	29	51	28	27	31	21	86	69	28	53	26	24	25	21	12	14
Zn	163	130	109	119	171	157	137	192	175	143	130	223	221	149	152	124
Ga	30	26	22	32	27	26	21	22	28	22	27	nm	nm	nm	nm	nm
Rb	59	59	86	214	83	122	63	105	184	93	222	78	78	nm	171	191
Sr	1299	1271	1150	1371	1178	348	1395	1120	758	884	507	1176	1168	nm	594	466
Y	53	37	50	11	36	12	60	34	61	69	54	50	37	48	55	65
Zr	361	401	622	317	304	59	147	178	623	423	550	385	388	50	722	746
Nb	27	24	23	31	22	18	25	26	29	25	26	55	57	nm	51	59
Ba	2232	1485	1337	2621	2287	833	2316	3358	992	1815	751	2842	2836	2277	2016	1882
Pb	nm	41	nm	nm	nm	nm	nm	31								

SA = Santa Angélica, CA = Castelo, PA = Pedra Azul. Data of SA and CA from Horn (1986); data of PA from Platzer (1997); Fe₂O₃-contents for Pedra Azul (PA) rocks correspond to Fe (total). nm = not measured.

In comparison to Santa Angélica, Castelo shows less plastic strain indicating different stress regimes and/or intrusion levels. Most of the magma-mingling features described in Santa Angélica (Schmidt-Thomé and Weber-Diefenbach, 1987; Wiedemann et al., 1997) are also observed in Castelo. In comparison to Santa Angélica, it lacks gabbro-noritic lenses interfingering the granites. In Castelo, granites interfinger dioritic and granodioritic rocks. Similar quartz xenocrysts with mafic rings, feldspars showing antirapakivi and rapakivi mantling (Hibbard, 1995) are also common features. Another typical sign for this hybrid zone are spotted textures and granitic schlieren in the microdiorite (Fig. 8f). Geochemical data of rocks from Castelo is presented as tables 2 and 3, and figures 10, 11 and 12.

Pedra Azul

The Pedra Azul Complex (PAC) is an irregular intrusion, that covers close to 200 km² and is formed by contrasting lithofacies grading from diorite to a medium-grained syenogranite (Fig. 6, Table 2; Costa-de-Moura et al., 1999). A general NW-SE and NE-SW fracturing is observed along the whole pluton and its enclosing rocks (sillimanite-quartzites and aluminous gneisses). The igneous

lithotypes are separated from the enclosing rocks by a migmatized zone, which shows stoping, *lit par lit* or nebulitic contacts, with widespread partial melting of the metamorphic units. Megaporphyritic or coarse-grained facies are absent from this intrusion. A medium-grained monzogranite builds or covers the highest peaks and lower border regions, constituting the first magmatic envelope of the structure. Several portions of tonalitic to granodioritic compositions were mapped towards the center of the structure. The contact between the monzogranite and the tonalitic to granodioritic domains is marked by mingled zones where granitic schlieren, in contact with more mafic- and finer-grained rocks, originate pillow-like and net-veined structures. A small region of dioritic composition is exposed over 6 km², at the northern border, close to the city of Aracê. The magmatic flow in the PAC is marked by a magmatic lineation clearly dipping 45° to the NE and the alignment of enclaves (Costa-de-Moura et al., 1999).

Abundant host rock slabs and smaller xenoliths of sillimanite-quartzites and garnet-sillimanite-biotite-gneisses form another hybrid lithology: an agmatitic mixture of granitic veins, cropping out over some 15 km, in a 1 km-wide zone. This zone follows a SE-NW lineament

Table 3. Chemical analyses of intermediate and acid rocks from Santa Angélica, Castelo and Pedra Azul, and from high-K calc-alkaline/alkaline rocks from Mimoso do Sul and Conceição de Muqui.

Sample	CA-6	CA-7	CA-8	PA-6	PA-7	SA-7	SA-8	SA-9	MI-1	MI-2	MI-3	MI-4	CM-1	CM-2	CM-3	CM-4
SiO ₂	66.97	72.12	72.44	67.02	71.57	71.81	76.20	72.45	64.81	56.55	46.66	38.11	71.34	66.05	52.27	45.83
TiO ₂	0.74	0.47	0.35	1.02	0.38	0.42	0.15	0.66	0.43	1.13	2.22	2.27	0.41	0.67	1.33	2.60
Al ₂ O ₃	15.28	13.81	13.30	14.26	13.71	13.86	12.44	11.87	17.39	17.29	12.35	9.02	13.36	14.33	15.69	15.72
FeO	3.68	2.31	1.45	nm	nm	1.36	0.71	2.62	1.51	4.30	5.66	10.31	1.41	2.36	3.41	5.99
Fe ₂ O ₃	0.65	0.41	0.97	4.97	2.98	0.90	0.47	0.46	0.55	2.35	4.62	4.93	1.04	0.69	2.67	5.10
MgO	1.45	0.78	0.42	0.87	0.44	0.69	0.36	0.84	0.42	3.70	7.30	10.28	0.18	1.02	2.98	6.01
CaO	2.40	1.46	1.49	2.54	1.14	2.68	1.00	1.84	2.32	5.37	7.42	14.78	1.75	3.22	3.20	7.41
Na ₂ O	2.13	1.49	1.94	2.89	2.57	3.34	3.93	2.83	2.83	1.81	4.59	1.69	2.83	4.23	4.03	2.57
K ₂ O	4.89	5.83	5.90	5.27	5.93	3.47	4.33	4.94	8.31	5.27	5.14	3.09	5.29	5.59	4.84	4.92
MnO	0.07	0.06	0.03	0.07	0.08	0.04	0.04	0.05	0.28	0.14	0.28	0.21	0.05	0.08	0.09	0.09
P ₂ O ₅	0.31	0.17	0.12	0.31	0.11	0.10	0.02	0.18	0.22	0.72	2.04	2.37	0.17	0.14	0.84	2.81
LOI	0.77	0.79	0.75	0.74	0.69	0.75	0.61	0.69	0.85	1.20	2.16	2.66	1.81	1.24	1.11	1.03
Total	99.34	99.70	99.16	99.97	99.60	99.42	100.26	99.43	99.92	100.1	100.4	99.72	99.74	99.65	99.49	100.1
Minor elements in ppm																
V	137	50	35	36	13	344	17	99	9	173	291	457	24	14	130	28
Cr	22	27	37	12	7	27	44	28	nm							
Co	12	4	5	23	29	40	1	12	2	14	42	93	4	2	7	15
Ni	18	36	34	8	5	20	71	17	nm							
Cu	22	25	22	7	2	36	32	26	6	37	66	55	3	28	31	72
Zn	127	143	101	91	64	114	275	99	124	94	67	106	128	80	162	127
Ga	22	24	23	nm	nm	24	21	19	23	78	21	65	27	21	26	24
Rb	200	219	185	291	260	68	107	130	201	145	102	6673	195	425	160	70
Sr	509	3335	585	229	179	1041	143	345	3001	2532	5001	2322	305	2070	1187	3215
Y	24	34	30	75	37	50	16	44	nm	52	79	73	25	2	56	41
Zr	395	438	321	749	323	309	149	446	369	758	478	323	325	385	612	272
Nb	21	18	16	52	34	24	2	17	nm							
Ba	1446	1039	1483	1354	927	1547	530	1230	nm	nm	nm	1640	nm	2471	6757	
Pb	37	56	52	30	35	19	26	19	nm							

SA = Santa Angélica, CA = Castelo, PA = Pedra Azul, CM = Conceição de Muqui, MI = Mimoso do Sul. Data of SA and CA from Horn (1986), data of MI from Wiedemann et al. (1986); data of CM from Murad (1992). Fe₂O₃-contents for PA rocks correspond to Fe (total). nm = not measured.

(fracture or fault zone), crosses almost the entire pluton and is probably an exploded and assimilated roof pendant from the uppermost part of the structure. Country rock xenoliths are also common along the border of this intrusion. Due to the limitations of the mapping scale such layers cannot be represented on the map. Nevertheless, several layers of country rock swarms were described parallel to the borders, in the granite domain. The last intrusive event in the PAGC was the emplacement of several stocks of ocellar syenogranite, which have been mapped along a NW-SE fracture zone. This late syenogranite shows a striking and peculiar texture formed by hololeucocratic spots, rich in titanite, wrapped by a biotite-magnetite-ilmenite-rich mesocratic matrix, in which allanite is also present.

Compared to other intrusive complexes, Pedra Azul has the largest volume of hybrid rocks. This may be explained by the different erosional levels. According to the magnetometric survey of this region (Tuller, 1993), the magnitude of the magnetic anomaly corresponding to the intrusion of Pedra Azul is very similar to the one for Santa Angélica. The small amount of outcropping basic rocks is probably due to differences in intrusion, erosion levels

and/or intensity of mingling or mixing. Geochemical data for rocks from Pedra Azul are presented as tables 2 and 3 and in figures 9, 10, 11 and 12.

Conceição de Muqui

The Conceição de Muqui Igneous Complex (Fig. 7) covers around 50 km² (Murad, 1992). In the eastern border area it is emplaced in coarse-grained biotite-hornblende porphyroblastic gneisses. In the northern and western borders it is emplaced into migmatitic gneisses and at the southern border into a finer-grained granodioritic to tonalitic orthogneissic sequence associated with amphibolites and banded migmatitic gneisses

The intrusive body consists of a series of transitional petrographic domains: (1) Mingling zone A, with incipient layering (at the central-eastern border), where medium-to coarse-grained monzodiorite dominates in a net-veined monzonite interfingered with the diorite; (2) Mingling zone B, with a strong planar flow (at the southern border), where a finer-grained diorite predominates over monzonite and is cross-cut by a network of coarse-grained leucogranitic to leucomonzonitic veins; (3) coarse-grained

leucomonzonite (mainly at the western border), is the most homogeneous unity of the intrusion, locally with a well marked flow structure and (4) medium to coarse-grained granitic rocks (mainly at the northern border), which basically corresponds to an increase of quartz content in the monzonite. The intrusion is cross-cut by syn-to-post-intrusive sills and dykes, with dioritic to granitic compositions; intermediate compositions are also present and the more felsic ones are the latest. These granitic dykes may be rich in enclaves and quartz-plagioclase-titanite-allanite orbicules.

The planar and/or linear flow structures are well preserved. Magmatic foliation dips sub-horizontally in the central part of the intrusion to sub-vertically in the border areas. Marginal radial shears are common. Country rock septa and xenoliths are abundant inside the intrusion and are commonly discordant with the flow structures. These observations suggest that the intrusive massif has a shallower erosion level than the Santa Angélica or Várzea Alegre plutons. The Conceição de Muqui intrusion represents a composition departure from the predominant high-K magmatism towards a quartz-poorer alkali-richer monzonitic series (Wiedemann, 1993; Table 3; Figs. 10, 11 and 12).

Mimoso do Sul

Mimoso do Sul is an intrusive complex (Fig. 7), that consists of two separated bodies: a monzonitic (Torre) and a gabbroic unit (Jacutinga). Torre is made of three concentric layers grading from a dioritic/monzodioritic center and a second ring of mesoperthitic monzonite to an outer ring of microcline-quartz-monzonite and granite. Leucomonzonites predominate at the contact to the enclosing rocks. The contact between the pluton and the enclosing rock is sharp. Inside the pluton there is a gradual changing from microcline-quartz-monzonite towards the dioritic/monzodioritic center and the separation of units followed petrographic criteria.

The gabbroic body of Jacutinga consists of gabbro-noritic rocks with compositions grading from fine-grained olivine-opx-cpx-melagabros up to coarse-grained opx-cpx-leucogabros. A fine igneous lamination is common in most Jacutinga gabbros consisting of a primary mineral orientation and coronitic textures with complex olivine-plagioclase contacts. This is only visible in boulders and could not be measured, due to the lack of outcrops. In Torre the magmatic foliation is steep to sub-vertical. Associated sills or dykes of peralkaline biotite-Fe-augite-apatite-pyroxenitic rocks cross-cut the outer border and the center of the intrusion.

The overall geochemical signature in Torre is high-K calc-alkaline to alkaline (Figs. 10, 11 and 12; Table 3).

The Jacutinga pluton has a different geochemical signature. It is tholeiitic, although strong enrichments in incompatible elements such as REE, Sr and Ba (Fig. 9) were reported by Wiedemann et al. (1995) and Ludka and Wiedemann (2000).

Summary of Observations

Late orogenic magmatism (535 to 480 Ma) in the Araçuaí-Ribeira Fold Belt is marked by the predominance of allanite-titanite-bearing granitoids. Smaller lenses of coronitic gabbro, anorthosite, pyroxenite and phlogopite-peridotite are seldom in this belt. The complexes shown here are I-type, generally emplaced along high-angle shear zones and antiformal fold hinges, that belong to the previous deformations (Figs. 3 and 4). The deep erosional level reveals the roots of these intrusions. These intrusions are the source of tourmaline-poor, beryl-rich pegmatites and the source for the most important production of dimension stones in Brazil.

The principal features of each intrusive complex were tabulated (Table 4). The complexes can be divided into: (1) an early charnockitic stage and (2) a late bimodal stage. The early charnockitic stage comprises coarse-grained, green-coloured hypersthene-bearing rocks that form batholiths, like those outcropping along the Doce river (latitude 19°30'), or that form units bordering younger intrusions (e.g., Várzea Alegre; Figs. 1 and 5, Table 1; Pinto et al., 1998; Mendes et al., 1999; Medeiros et al., 2000). The late bimodal stage is the youngest post-collisional magmatic episode, which is marked by several igneous complexes with compositions varying from gabbro to granite. Local names for this suite are Pedra Azul, Santa Angélica, Castelo, Iconha, Venda Nova, Conceição de Muqui, Mimoso do Sul and Várzea Alegre (Figs. 1, 4, 5, 6 and 7). Finer-grained biotite granodiorite, biotite monzo-to syenogranite are late facies intruded as stocks, dykes, and sills and, in some places, form the uppermost portion of the plutons. The deep erosional level associated with a steep topography exposes: funnel-like bodies with sub-vertical cylindrical roots, grading to tabular tops. In the horizontal section shapes are nearly elliptical, ameboid or rounded. Associated stocks, sills and mostly dykes of basic and acid magmas intrude the enclosing gneisses along the foliation, local ductile shear zones and fold axes. The contact with these enclosing rocks is sharp in deeper eroded plutons (Santa Angélica, Venda Nova and Várzea Alegre). Up to 100 m narrow migmatic nebulitic zones are found in the contact area. Where supposed higher levels are exposed (Castelo, Pedra Azul and Conceição de Muqui), agmatic to nebulitic zones are up to 4 km wide. The igneous foliation is usually well-developed and the

Table 4. Sm–Nd isotopic results for country rocks (AS-1, kinzigite, and IR-3, enderbite) and magmatic rocks of the studied plutons. VA-218 and VA-269, opx-gabbros; SA-50, granite; SA-51, granite; SA-71a, SA-72 and SA-63, gabbrodiorites.

Sample	AS -1	IR-3	VA-218	VA-269	SA-50	SA-51	SA-71-A	SA-72	SA-63
Sm (ppm)	8.958	5.033	6.866	11.477	11.55	24.296	17.908	18.449	20.931
Nd (ppm)	41.773	26.14	41.867	70.094	85.74	173.21	121.61	118.56	137.9
$^{143}\text{Nd}/^{144}\text{Nd}$	0.511997±19	0.512007±30	0.512047 (28)	0.512002 (24)	0.511599±05	0.511575±11	0.511600±13	0.511608±16	0.511625±19
$^{147}\text{Sm}/^{144}\text{Nd}$	0.1296	0.1164	0.099795 (71)	0.099633 (84)	0.0814	0.0848	0.0890	0.0941	0.0918
T _{DM} (Ga)	1,881	1,608	1,329	1,383	1,653	1,723	1,751	1,816	1,760
T (Ga)	0,55	0,55	0,55	0,55	0,55	0,55	0,55	0,55	0,55
Epson (0)	-12.50	-12.31	-11.53	-12.41	-20.27	-20.74	-20.25	-20.09	-19.76
Epson (T)	-7.80	-6.67	-4.73	-5.59	-12.18	-12.89	-12.70	-12.90	-12.40
$^{143}\text{Nd}/^{144}\text{Nd}_{\text{di}}$	0.511530	0.511588	0.511687	0.511643	0.511306	0.511268	0.511279	0.511269	0.51129

VA= Várzea Alegre, SA= Santa Angelica. Source of data: Medeiros and Wiedemann (subm.).

schistosity of the surrounding gneisses wraps around the plutons. Crenulation of the primary igneous foliation was observed only in the southern border of Santa Angélica. Each intrusion has an unique marble cake (bimodal) internal structure: concentric patterns of more basic to intermediate cores are surrounded by interfingered lenses of basic to acid plutonic rocks. Syenomonzonite and granite predominate in the borders. Widespread evidence of mingling between contrasting magmas of gabbroic and granitic or syenomonzonitic composition is present in all intrusive complexes.

Review of Geochemical and Geochronological Data

Whole-rock geochemical analysis point towards the existence of three magmatic suites: a tholeiitic, a calc-alkaline and an alkaline (Tables 1, 2 and 3; Figs. 10, 11 and 12; Wiedemann, 1993). The calc-alkaline suite is the most significant and comprises ~90% of all plutons by area in the southern region. This suite comprises metaluminous (Fig. 12), high-K calc-alkaline (Fig. 10 and

12) granitoids originated in the continental crust, but with an important enriched mantle contribution (Fig. 9, Tables 5 and 6; Mendes et al., 1997, 1999; Ludka et al., 1998; Medeiros et al., 2001; Medeiros and Wiedemann, 2001).

Geobarometric studies point towards pressures ranging from 5.9 to 11.5 kb (Tables 7 and 8). Rb–Sr and Sm–Nd isotopic data (Tables 5 and 6; Medeiros et al., 2000) and the geochemical signatures (Wiedemann et al., 1995; Ludka et al., 1998) indicate an enriched and crustal contaminated mantle source for the basic and intermediate rocks of this suite. In tables 5 and 6 the values of ϵ_{Nd} for the young basic rocks from Várzea Alegre and Santa Angélica are abnormally negative. In the case of Santa Angélica gabbros, the values obtained are more negative than those measured in the enclosing metasediments. The calculated CHUR model age (related to the time of the last extracting event from the mantle source) is around 1 Ga and may reflect an episode of mantle enrichment (mixing between juvenile mantle and crust), probably related to the rift phase connected to the opening of the Adamastor-Brazilides ocean (Pedrosa-Soares et al., 1998). From around 530 to 480 Ma a

Table 5. Whole-rock Rb–Sr analytical results of rocks from Várzea Alegre.

Sample	Rock type	Rb (ppm)	Sr (ppm)	$^{87}\text{Rb}/^{86}\text{Sr}$	Error	$^{87}\text{Sr}/^{86}\text{Sr}^{(\text{f})}$	Error	$^{87}\text{Sr}/^{86}\text{Sr}^{(\text{i})}$	$\epsilon_{\text{Sr}}^{(\text{0})}$	$\epsilon_{0.55\text{GaSr}}^{**}$
VA-06 (D)	Quartz-diorite	53.24	955.61	0.1613	0.0024	0.708330	0.000080	0.707065	47.23	45.66
VA-18 (F)	Qtz -monzonite	50.79	1300.86	0.1130	0.0018	0.707420	0.000130	0.706534	34.32	38.12
VA-218 (G)	Opx-gabbro	15.71	1033.81	0.0440	0.0006	0.707610	0.000080	0.707265	37.02	48.50
VA-269 (D)	Opx-gabbro	34.52	1108.48	0.0901	0.0013	0.707120	0.000130	0.706414	30.07	36.41
VA-204 (E)	Granite	204.20	182.60	3.2440	0.0920	0.731560	0.000160	0.706125	-	32.31
VA-176	Granite	242.20	155.30	4.5280	0.1280	0.740730	0.000110	0.705228	-	19.56
VA-204a	Granite	159.60	365.60	1.2650	0.0360	0.717530	0.000060	0.707612	-	53.43
VA-04 (B)	Charnoenderbite	109.80	666.20	0.4770	0.0130	0.715390	0.000190	0.711650	147.37	110.80
VA-257 (C)	Charnoenderbite	59.79	665.12	0.2602	0.0037	0.710740	0.000160	0.708700	81.41	68.89
VA-249 (C)	Charnoenderbite	75.61	674.14	0.3262	0.0050	0.711980	0.000120	0.709422	99.01	79.15

Values obtained from following equations:

$$\epsilon_{\text{Sr}}^{(0)} = \frac{[\text{Sr}^{87}/\text{Sr}^{86} - 1] \times 10^4}{0.7045}$$

$$\epsilon_{0.55\text{GaSr}}^{**} = \frac{[\text{Sr}^{87}/\text{Sr}^{86}]^{(\text{i})} - 1]{[\text{Sr}^{87}/\text{Sr}^{86}]^{(\text{f})}} \times 10^4$$

Table 6. Microprobe analyses of amphiboles.

	I-0984a*	I-0984b*	VA-202*	VA-06*	VA-261**	StA (R410a)**	StA (R410b)**
SiO ₂	43.14	42.88	41.99	42.77	40.02	42.76	42.13
TiO ₂	1.20	1.11	1.20	1.72	2.22	1.39	1.38
Al ₂ O ₃	10.25	10.06	10.10	11.09	11.13	10.23	9.37
Cr ₂ O ₃	0.20	nd	nd	nd	nd	0.02	nd
Fe ₂ O ₃	3.70	3.83	nd	nd	nd	nd	nd
FeO	17.16	17.15	18.79	16.82	21.11	17.73	17.57
MnO	0.35	0.30	0.57	0.35	0.28	0.34	0.35
MgO	8.41	8.22	9.27	10.44	7.14	10.95	11.21
CaO	10.51	10.32	11.10	11.53	11.86	11.46	11.94
Na ₂ O	1.39	1.38	1.57	1.16	1.11	1.49	1.58
K ₂ O	1.18	1.09	1.57	1.53	1.68	1.34	1.31
Total	96.94	95.96	96.15	97.41	96.55	97.76	96.84
Si	6.511	6.538	6.475	6.421	6.247	6.46	6.40
Al ^{IV}	1.493	1.474	1.525	1.579	1.753	1.54	1.590
Al ^{VI}	0.342	0.349	0.310	0.381	0.293	0.28	0.80
Fe ⁺²	2.174	2.195	2.088	1.778	2.470	1.95	1.75
Fe ⁺³	0.428	0.442	0.335	0.334	0.286	0.24	0.48
Mg	1.896	1.871	2.131	2.336	1.661	2.46	2.54
Mn	0.049	0.041	0.046	0.044	0.029	0.04	0.04
Ti	0.143	0.132	0.191	0.194	0.261	0.16	0.16
Ca-B	1.730	1.693	1.885	1.854	1.983	1.86	1.94
Na-B	0.322	0.311	0.061	0.078	0.009	0.0	0.0
K-A	0.234	0.214	0.318	0.293	0.335	0.26	0.25
Na-A	0.112	0.091	0.302	0.260	0.327	0.44	0.46

*Formula units based on 24 (O, OH, F, Cl), **Formula units based on 23 (O, OH, F, Cl), nd= not detected, samples I-0984 from Offman (1990), samples VA- from Medeiros (1999), samples StA from Schmidt-Thomé (1989).

Table 7. Geobarometric calculations (in kb), using Al-contents in amphiboles, for samples from Iconha, Várzea Alegre and Santa Angélica.

Sample	H and Z (1986)	Schmidt (1992)	Anderson and Smith (1995)
I-0984	5.3 (1)		
I-0984	5.3 (1)		
VA-06		6.6±0.6 (2)	6.61±0.6 (T = 980°C) (4)
VA-202		5.7±0.6 (2)	5.53±0.6 (T = 980°C) (4)
VA-261.1		6.7±0.6 (3)	
StA (410A)			5.96±0.6 (T = 720°C) (4)
StA (410B)			11.47±0.6 (T= 720°C) (4)

StA (410) = Allanite-granite, VA-06/202 = quartz-diorite, VA 261 = Charnockite, I-0984 = quartz-diorite, (1) Offman, 1990, (2) Medeiros (1999), (3) Mendes et al. (1999), (4) new data; calculations followed the methods of H and Z = Hammarstrom and Zen (1986); Schmidt (1992) and Anderson and Smith (1995).

progressive increase in the amount of mantellic melts mixed with crustal melts suggests an important mechanism of underplating (Mendes et al., 1999; Medeiros et al., 2000; Medeiros and Wiedemann, in review).

Zircon ages constrain the magmatic crystallization of the late plutons from ca. 530 to 480 Ma confirming their late-orogenic origin (Söllner et al., 2000). Units from the Santa Angélica and Mimoso do Sul Complexes gave the following U-Pb ages: 513± 8 Ma for the megaporphyritic granite of Santa Angélica, 492±15 Ma for the type-II titanite-granite of Santa Angélica and 480± 4 Ma for the

coarse grained monzonite of Mimoso do Sul. Rb-Sr data from the megaporphyritic granite from Várzea Alegre yield a whole-rock isochron age of 508±12 Ma. with ⁸⁷Sr/⁸⁶Sr initial ratio of 0.7084, which is an evidence of crustal origin (Wiedemann et al., 1995; Medeiros et al., 2000). Whole-rock Rb/Sr isotopic data, obtained by Platzer (1997) from samples of Pedra Azul indicate a crystallization age of 536± 31 Ma for the granite of this pluton.

Along the whole fold belt, the post-collisional magmatism becomes progressively younger from northern Minas Gerais towards southern Espírito Santo. The time span of the whole late- to post-collisional arc-shaped magmatism lasted for 100 Ma (from 580 to 480 Ma). Based on several structural and geological evidence (Bayer, 1987; Lammerer, 1987; Pedrosa-Soares and Wiedemann-Leonardos, 2000), we assume that, during this period, there was a gradual change from a contractional towards a relaxation and an extensive tectonic regime along the central and northern part of the mobile belt.

Conclusions

Mechanisms of ascent and emplacement of plutons may be grouped into two main categories, according to Castro and Fernandez (1998): (a) permissive mechanism, in which

Table 8. Principal features of the intrusive complexes.

Pluton	Principal rock types	Country rocks and contacts relations	Shape and internal structure	Mingling textures and features	Age	Estimated depth of emplacement
Várzea Alegre	Opx-cpx-gabbro/monzogabbro + coarse and fine grained granites	High amphibolite to granulite gneisses	Roughly circular, outer charnockitic domain, inner domain inversely zoned	Dioritic pillow-like structures in granite, mantled feldspars	508 +/-8 Ma, Rb-Sr whole-rock	15 to 20 km
Santa Angélica	Opx-cpx-gabbro/monzogabbro + coarse and fine grained granites	High amphibolite gneisses	Elliptical, gabbroic twin core, inversely zoned	Gabbro-dioritic enclaves swarms, bimodal dykes, mantled feldspars and coronas	513 +/-8 Ma, 492 +/-15, U-Pb in zircons	15 to 20 km
Castelo	Diorite, granodiorite, coarse and fine grained granites	High amphibolite gneisses	Elliptical, dioritic core with thin microdioritic layer at contact to coarse granite	Dioritic enclaves swarms, cross joints filled with granite, mantled feldspars	No data	~<15 km
Pedra Azul	Granodiorite, tonalite and fine grained granites; diorite restricted	Sillimanite-quartzites and paragneisses (kinzigite)	Ameboidal shaped	Pillow-like and net-veined mingled zones, mantled feldspars	536 +/-31 Ma, Rb-Sr whole-rock	~<15 km
Conceição de Muqui	Diorite, monzonite, coarse and fine grained granites	High amphibolite ortho-gneisses	Egg shaped abundant country rock septa in the monzogranitic domains	Net-veined and pillow-like mingling, mantled feldspars	No data	~15 km
Mimoso do Sul	Syenomonzonite and monzodiorite. Granite restricted	High amphibolite gneisses	Egg shaped to circular, inversely zoned.	Mantled feldspars, coronas, bimodal dykes	480 +/-4 Ma, U-Pb in zircons	~15 km

the magma plays a passive role (stoping, accommodation in extensional faults) and (b) forceful mechanism, in which the magma pushes aside the pluton walls and deforms the country rocks creating by itself the room it will occupy (diapirism and ballooning).

From the data summarized from the literature and the observations described here we conclude that:

- 1) These six plutons clearly cut the regional enclosing rocks. The latest deformational phases in the region were dated around 580 Ma while the plutons crystallized around 510 to 480 Ma;
- 2) They all show border foliations which are concordant with the enclosing rocks in the border regions. Magma is squeezed into the enclosing foliation or may cut it along ductile shear zones or dykes;
- 3) They all intrude along contact zones between two different regional lithologies, along fold hinges or shear zones, using the regional weakness and deformational features as preferable paths. Nevertheless, their intrusion is not coeval with regional deformation; implying that it does not seem to have resulted from a mechanism of tectonic pumping, such as the typical post-collisional syntectonic emplacement (see Brown and Solar, 1999);

- 4) Their overall shape is cylindrical to balloon-like with nebulitic to agmatitic border zones, which could be indicative of a mixed mechanism;
- 5) This more or less extensive migmatization around the contacts underlines a more complex mechanism for making room by local ductile deformation and coeval partial melting of the enclosing rocks.

The summarized data suggests that these complexes were neither emplaced through a simple permissive dyking nor a simple forceful ballooning mechanism. In the present case the structures are controlled by rock weakness zones, such as regional foliation, shear zones and fault hinges. The whole magmatic evolution was a very slow process, which took over 50 Ma within a long-lasting highly viscous hot crust. This would rather suggest a more complex mechanism of magma migration in hot country rocks, such as the one proposed by Weinberg (1999). The gap between the main deformational phase (600–580 Ma) and this late orogenic magmatism (ca. 500 Ma) is relatively large for a direct connection. On the other hand, the spatial distribution of this magmatism is parallel to the strike of the older orogenic magmatism. This suggests some correlation. A possible explanation could be a delamination and break-off of the lithospheric mantle slab

causing relaxation and hot asthenospheric mantle emplacement.

Therefore, we propose the following model (Fig. 13): (1) replacement of lithospheric mantle by hot asthenospheric mantle, following collisional orogenesis; (2) induced crustal partial melting, which produced granitic and monzonitic melts; (3) interaction of these contrasting magmas, originating bimodal magma channels and (4) emplacement of composite plutons along older regional structures, such as regional fold hinges and ductile shear zones. The different compositions that were mapped are most likely explained by different degrees of interaction of the contrasting magmas, differentiation processes during ascent, emplacement and erosional levels.

Acknowledgments

We are grateful to several financing agencies: CNPq, FINEP, CAPES and DAAD. The results presented have important contributions from many undergraduate and graduate students, a list too long to be named here. Special thanks to Roberto Weinberg, Ricardo da Costa Nascimento and Amin Murad for their work in Castelo, Pedra Azul and Conceição de Muqui. To them all, we express our deepest recognition. The local population of all the areas under study, helped the students and researchers with lodging, additional care, nice coffee and fresh water breaks. We are equally grateful for the helpful contribution of Bernd Lammerer and Othon Leonardos, and to the very stimulating critical comments from the reviewers of this manuscript, Mike Brown and Roberto Weinberg, who helped us in polishing the first version of this work. Nevertheless, the authors remain totally responsible for any inconsistencies.

References

- Anderson, J.L. and Smith, D.R. (1995) The effects of temperature and f_{O_2} on the Al-in-horblenda barometer. Amer. Mineral., v. 80, pp. 549-559.
- Bayer, P. (1987) Strukturgeologische Untersuchungen im brasilianischen Küsten Mobile Belt, südliches Espírito Santo, unter Berücksichtigung der Brasiliano Intrusionen. Münchner Geowiss. Abh. v. 2, 80p.
- Bayer, P., Schmidt-Thomé, R., Weber-Diefenbach, K. and Horn, H.A. (1987) Complex concentric granitoid intrusions in the coastal mobile belt, Espírito Santo, Brazil: the Santa Angélica Pluton—an example. Geol. Rund., v. 76, pp. 357-371.
- Bosum, W. (1973) O levantamento aeromagnético de Minas Gerais e Espírito Santo e sua seqüência quanto a estrutura geológica. Rev. Bras. Geoc., v. 3, pp. 149-163.
- Brown, M. (1994) The generation, segregation, ascent and emplacement of granite magma: the migmatite-to-crystallly-derived granite connection in thickened orogens. Earth Sci. Rev., v. 36, pp. 83-130.
- Brown, M. (1995) Late-Precambrian geodynamics evolution of the Armorican segment of the Cadomian Belt (France): distortion of an active continental margin during south-west directed convergence and subduction of a bathymetric high. Geol. de la France, v. 3, pp. 3-22.
- Brown, M. and Solar, G.S. (1999) The mechanism of ascent and emplacement of granite magma during transpression: a syntectonic granite paradigm. Tectonophys., v. 312, pp. 1-33.
- Castro, A. and Fernández, C. (1998) Granitic intrusion by externally induced growth and deformation of the magma reservoir, the example of the Plasenzuela pluton, Spain. J. Struct. Geol., v. 20, pp. 1219-1228.
- Clemens, J.D. and Mawer, C.K. (1992) Granitic magma transport by fracture propagation. Tectonophys., v. 204, pp. 339-360.
- Collins, W.J. and Sawyer, E.W. (1996) Pervasive granitoid magma transfer through the lower-middle crust during non-coaxial compressional deformation. J. Metam. Geol., v. 14, pp. 565-579.
- Costa, A.G. (1998) The granulitic-facies rocks of the northern segment of the Ribeira Belt, eastern Minas Gerais, SE Brazil. Gondwana Res., v. 1, pp. 367-372.
- Costa-de-Moura, J., Wiedemann, C.M., Wallfass, C.M. and Van Westrenen, W. (1999) O Plutón de Pedra Azul: a estrutura do maciço intrusivo e suas rochas encaixantes – Domingos Martins, Espírito Santo, Brasil. In: VII Simpósio Nacional de Estudos Tectônicos – Simp. Int. de Tectônica da SBG, Lençóis (Ba). Anais, pp. 129-131.
- Cunningham, W.D., Alkmin, F.F. and Marshak, S. (1998) A structural transect across the coastal mobile belt in the Brazilian highlands (latitude 20°S): the roofs of a Precambrian transpressional orogen. Precamb. Res., v. 92, pp. 251-275.
- Fischel, D.P. (1998) Geologia e dados isotópicos Sm-Nd do Complexo Mantiqueira e do Cinturão Ribeira na região de Abre Campo, Minas Gerais. Inst. Geoc., Univ. de Brasília, M.Sc. dissertation, 99p.
- Fritzer, T. (1991) Das Guaçuí Lineament und die orogene Entwicklung des Zentralen Ribeira Belt (Espírito Santo, Brasilien). Münch. Hef., v. 2, 196p.
- Hammarstrom, J.M. and Zen, E-an (1986) Aluminium in hornblende: an empirical igneous geobarometer. Amer. Mineral., v. 71, pp. 1297-1313.
- Haralyi, N.L.E. and Hasui, Y. (1982) The gravimetric information and the Archean-Proterozoic struttural framework of eastern Brazil. Rev. Bras. Geoc., v. 12, pp. 160-166.
- Heilbron, M., Duarte, B.P. and Nogueira, J.R. (1998) The Juiz de Fora Complex of the Central Ribeira belt, SE Brazil: a segment of Paleoproterozoic granulitic crust thrusted during the Pan-African Orogen. Gondwana. Res., v. 1, pp. 373-382.
- Hibbard, M.J. (1995) Petrography to petrogenesis. Prentice Hall, Inc., 587p.
- Hongan, J.P., Price, J.D. and Gilbert, M.C. (1998) Magma traps and driving pressure: consequences for pluton shaped and emplacement in an extensional regime. J. Struct. Geol., v. 20, pp. 1155-1169.
- Horn, H.A. (1986) Plutonite in Espírito Santo. Geochemische Untersuchungen an Intrusivkomplexen des Brasiliano im Kuestengürtel von Espírito Santo / Brasilien. Unpublished Ph.D thesis. Inst. F. Allg. U. Angew. Geol. Der LMU. Munich, Germany, 187p.

- Irvine, T.N. and Baragar, W.R. (1971) A guide to chemical classification of the common volcanic rocks. *Can. J. Earth Sci.*, v. 8, pp. 523-548.
- Lammerer, B. (1987) Short notes in a structural section through the Ribeira Mobile Belt (Minas Gerais and Espírito Santo, Brazil). *Zbl. Geol. Paläont. Teil I*, v. (7/8), pp. 719-728.
- Ludka, I.P. (1991) *Geologia, Petrografia e Geoquímica do Complexo Intrusivo de Jacutinga-Torre-Mimoso do Sul, Espírito Santo*. Master Thesis (Unpub.), Federal University of Rio de Janeiro/UFRJ/Brazil, 110p.
- Ludka, I.P., Wiedemann, C.M. and Töpfner, C. (1998) On origin of incompatible element in the Venda Nova pluton, state of Espírito Santo, southeast Brazil. *J. South Amer. Earth Sci.*, v. 11, pp. 473-486.
- Ludka, I.P. and Wiedemann, C.M. (2000) Further signs of an enriched mantle source under the Neoproterozoic Araçuaí-Ribeira Mobile Belt. Brazilian contributions to the 31st International Geological Congress, Brazil/2000. *Rev. Bras. Geoc.*, v. 30, pp. 95-98.
- Machado, N., Valladares, C., Heilbron, M. and Valeriano, C.M. (1996) U-Pb Geochronology of the Central Ribeira Belt (Brazil) and implications for the evolution of the Brazilian orogeny. *Precamb. Res.*, v. 79, pp. 347-361.
- Maniar, P.D. and Piccoli, P.M. (1989) Tectonic discrimination of granitoids, *Geol. Soc. Amer. Bull.* v. 101, pp. 635-643.
- Marre, J. (1986) The structural analysis of granite rocks. North Oxford Acad. Publ. Great Britain, 123p.
- Medeiros, S.R. (1999) *Estudo Mineralógico, Petrográfico, Geoquímico e Isotópico do Complexo Intrusivo de Várzea Alegre - ES*. Ph.D. Thesis (Unpub.), Instituto de Geociências, Universidade Federal do Rio de Janeiro, 174p.
- Medeiros, S.R., Wiedemann, C.M. and Mendes, J.C. (2000) Post-collisinal magmatism in the Ribeira Mobile Belt: geochemical and isotopic study of the Várzea Alegre Intrusive Complex (VAIC), ES, Brazil. Brazilian contributions to the 31st International Geological Congress, Brazil/2000. *Rev. Bras. Geoc.*, v. 30, pp. 30-34.
- Medeiros, S.R., Wiedemann, C.M. and Vriend, S. (2001) Evidence of mingling between contrasting magmas in a deep plutonic environment: the example of Várzea Alegre, in the Pan-Africa/Brasiliano Mobile Belt in Brazil. *An. Acad. Bras. Ci.*, v. 73, pp. 99-119.
- Medeiros, S.R. and Wiedemann, C.M. (2001) New Sm-Nd isotopic data from the southern Araçuaí-Ribeira Belt: Paráiba do Sul group and associated granitic intrusions. International Geochronological Meeting, Chile. October, 2001.
- Mendes, J.C., McReath, I., Wiedemann, C.M. and Figueiredo, M.C.H. (1997) Charnoquítoides do Maciço de Várzea Alegre: um exemplo de magmatismo cálcio-alcalino de alto K no arco magmático do espírito Santo. *Rev. Bras. Geoc.*, v. 27, pp. 13-24.
- Mendes, J.C., Wiedemann, C.M. and McReath, I. (1999) Conditions of formation of charnockitic magmatic rocks from the Várzea Alegre massif, Espírito Santo, southeast Brazil. *Rev. Bras. Geoc.*, v. 29, pp. 47-54.
- Meneses, P.R. and Paradella, W.R. (1978) Síntese geológica preliminar da parte sul do Estado do Espírito Santo. In: Simpósio Brasileiro De Sensoriamento Remoto, 1978, São José dos Campos (SP). Anais, São José dos Campos, INPE/CNPq, pp. 479-499.
- Murad, A. (1992) *Geologia, Petrografia e Geoquímica (Elementos Maiores, Menores e alguns Traços) do Maciço Intrusivo de Conceição de Muqui, Espírito Santo*. Master Thesis (Unpub.), Federal University of Rio de Janeiro/UFRJ/Brazil, 98p.
- Offman, R. (1990) Geologische, petrographische und geochemische charakterisierung des Intrusivkomplexes von Iconha im südlichen Espírito Santo, Brasilien, sowie petrogenetisch interpretation. Ph.D. Thesis (Unpub.), LMU, Munich, Germany, 190p.
- Pedrosa-Soares, A.C., Vidal, P., Leonards, O.H. and Brito-Neves, B.B. (1998) Neoproterozoic oceanic remnants in eastern Brazil: further evidence and refutation of an exclusively ensialic evolution for the Araçuaí-West Congo orogen. *Geology*, v. 26, pp. 519-522.
- Pedrosa-Soares, A.C., Wiedemann, C.M., Fernandes, M.L.S., Faria, L.F. and Ferreira, J.C.H. (1999) Geotectonic significance of the Neoproterozoic granitic magmatism in the Araçuaí Belt, eastern Brazil: a model and pertinent questions. *Rev. Bras. Geoc.*, v. 29, pp. 59-66.
- Pedrosa-Soares, A.C. and Wiedemann-Leonards, C.M. (2000) Evolution of the Araçuaí Belt and its connection to the Ribeira Belt, eastern Brazil. In: Cordani, U. (Ed.), *Tectonic evolution of South America. 31st IGC*, pp. 265-285.
- Pedrosa-Soares, A.C., Noce, C.M., Wiedemann, C.M. and Pinto, C.P. (2001) The Araçuaí-West Congo Orogen in Brazil: an overview of confined orogen formed during Gondwana assembly. *Precamb. Res.*, v. 110, pp. 307-323.
- Petford, N., Lister, J.R. and Kerr, R.C. (1994) The ascent of felsic magmas in dykes. *Lithos*, v. 32, pp. 161-168.
- Pinto, C.P., Pedrosa-Soares, A.C. and Wiedemann, C.M. (1998) Mapa Geológico da porção brasileira do Orógeno Araçuaí-Oeste-Congo. SBG, Congresso Brasileiro de Geologia, 40, Belo Horizonte, p. 37 (abst.).
- Platzer, S. (1997) Whole-rock geochemistry of the Aracê/Pedra Azul pluton. Unpublished M. S. thesis, University of Utrecht, The Netherlands, 58p.
- Roig, J.Y., Faure, M. and Truffert, S.R. (1998) Folding and granite emplacement inferred from structural, strain, TEM and gravimetric analyses: the case study of the Tulle antiform, SW French Massif central. *J. Struct. Geol.*, v. 20, pp. 1169-1190.
- Schmidt, M.W. (1992) Amphibole composition in tonalite as a function of pressure: an experimental calibration of the Al-in-hornblende barometer. *Contrib. Mineral. Petrol.*, v. 110, pp. 304-310.
- Schmidt-Thomé, R. and Weber-Diefenbach, K. (1987) Evidence for 'frozen-in' magma mixing in Brasiliano calc-alkaline intrusions. The Santa Angélica pluton, southern Espírito Santo, Brazil. *Rev. Bras. Geoc.*, v. 17, pp. 498-506.
- Schmidt-Thomé, R. (1989) Der Santa Angélica Pluton in Ribeira Belt, südliches Espírito Santo, Brasilien. Magmenmischung in einem invers zonierten Pluton. Ph.D. Thesis (Unpub.), LMU, Munich, Germany, 180p.
- Seidensticker, U. and Wiedemann, C.M. (1992) Geochemistry and origin of lower crustal granulite facies rocks in the Serra do Caparaó region, Esp.Santo/Minas Gerais, Brazil. *J. South Amer. Earth Sci.*, v. 6, pp. 289-298.
- Söllner, F., Lammerer, B. and Wiedemann-Leonards, C.M. (2000) Dating the Ribeira Mobile Belt of Brazil. In: Sonderheft, Zeit. f. Angw. Geol., Hannover/2000, pp. 245-255.

- Sun, S.S. and McDonough, W.F. (1989) Chemical and isotopic systematic of oceanic basalts: implications for mantle composition and processes. In: Saunders, A.D. and Norry, M.J. (Eds.), *Magmatism in the ocean basins*, Geol. Soc. London, Spl. Publ., v. 42, pp. 313-345.
- Tuller, M.P. (1993) Texto Explicativo da Folha SE. 24-Y-C-VI, Colatina. In: Tuller, M.P. (org.), *Programa Levantamentos Geológicos Básicos do Brasil*, DNPM/CPRM Brasília. 163p.
- Weinberg, R.F. and Podladchikov, Y. (1994) Diapiric ascent of magmas through power-law crust and mantle. *J. Geophys. Res.*, v. 99, pp. 9543-9559.
- Weinberg, R.F. (1999) Mesoscale pervasive felsic magma migration: alternatives to dyking. *Lithos*, v. 46, pp. 394-410.
- Wiedemann, C.M., Bayer, P., Horn, H., Lammerer, B., Ludka, I.P., Schmidt-Thomé, R. and Weber-Diefenbach, K. (1986) Maciços intrusivos do Espírito Santo e seu contexto regional. *Rev. Bras. Geoc.*, v. 16, pp. 24-37.
- Wiedemann, C.M. (1993) The evolution of the early Paleozoic late- to Post-Collisional Magmatic Arc of the Coastal Mobile Belt in the State of Espírito Santo, eastern Brazil. *An. Acad. Bras. Cienc.*, v. 5, pp. 163-181.
- Wiedemann, C.M., Mendes, J.C. and Ludka, I.P. (1995) Contamination of mantle magmas by crustal contributions – evidence from the Brasiliano Mobile Belt in the State of Espírito Santo, Brazil. *An. Acad. Bras. Cienc.*, v. 67, pp. 279-292.
- Wiedemann, C.M., Mendes, J.C., Costa-de-Moura, J., Costa-Nascimento, R. and Ludka, I.P. (1997) Granitoids of the Espírito Santo Magmatic Arc. SBG, International Symp. on granites and associated mineralizations, 2 Excursions Guide, pp. 57-76.